

# Sparse online variational Bayesian regression

Kody J.H. Law\*      Vitaly Zankin\*

December 23, 2021

## Abstract

This work considers variational Bayesian inference as an inexpensive and scalable alternative to a fully Bayesian approach in the context of sparsity-promoting priors. In particular, the priors considered arise from scale mixtures of Normal distributions with a generalized inverse Gaussian mixing distribution. This includes the variational Bayesian LASSO as an inexpensive and scalable alternative to the Bayesian LASSO introduced in [65]. It also includes a family of priors which more strongly promote sparsity. For linear models the method requires only the iterative solution of deterministic least squares problems. Furthermore, for  $p$  unknown covariates the method can be implemented exactly online with a cost of  $\mathcal{O}(p^3)$  in computation and  $\mathcal{O}(p^2)$  in memory per iteration – in other words, the cost per iteration is independent of  $n$ , and in principle infinite data can be considered. For large  $p$  an approximation is able to achieve promising results for a cost of  $\mathcal{O}(p)$  per iteration, in both computation and memory. Strategies for hyper-parameter tuning are also considered. The method is implemented for real and simulated data. It is shown that the performance in terms of variable selection and uncertainty quantification of the variational Bayesian LASSO can be comparable to the Bayesian LASSO for problems which are tractable with that method, and for a fraction of the cost. The present method comfortably handles  $n = 65536$ ,  $p = 131073$  on a laptop in less than 30 minutes, and  $n = 10^5$ ,  $p = 2.1 \times 10^6$  overnight.

## 1 Introduction

Regression is a quintessential and ubiquitous task of machine learning. The simplest method one can use to solve regression tasks is a linear model with Gaussian noise and prior [11]. The most attractive feature of linear Gaussian models is analytical tractability, from both frequentist and Bayesian viewpoints. However, once one employs basis function expansions, they also become quite flexible. There are numerous methods in which linear models can be embedded, such as total least squares [87] and mixtures of regressions [50], for example. Sparsity promoting priors have proven to be very useful for identifying useful features and avoiding overfitting, perhaps most notably the LASSO [81] and its incarnation as total variation (TV) regularization in imaging [84, 79]. However, as soon as a non-Gaussian prior is introduced then analytical tractability is lost and, in particular, the Bayesian solution becomes very expensive [65], requiring Markov chain Monte Carlo (MCMC) methods [71, 41]. Furthermore, sparsity promoting priors are not differentiable, which prevents the use of simple Gaussian approximations such as Laplace approximation [7].

---

\*Department of Mathematics, University of Manchester, UK.

## 1.1 Linear models

Let  $\mathcal{D}_n = \{(x_i, y_i)\}_{i=1}^n$ , with  $x_i \in \mathbb{R}^p$  and  $y_i \in \mathbb{R}$  (for simplicity), and let  $X_n = [x_1, \dots, x_n]^T$  and  $Y_n = (y_1, \dots, y_n)^T$ . Consider the following statistical model, in a Bayesian linear regression context

$$y_i = x_i^T \beta + \epsilon_i, \quad \beta \perp \epsilon_i \sim N(0, \gamma^2) \text{ i.i.d. for } i = 1, \dots, n, \quad (1)$$

where  $N(m, C)$  denotes a multivariate Gaussian distribution with mean  $m \in \mathbb{R}^l$ ,  $l \geq 1$ , and covariance  $C \in \mathbb{R}^{l \times l}$ . The notation  $N(z; m, C)$  will be used to denote the corresponding density with argument  $z \in \mathbb{R}^l$ . The Bayesian formulation of this problem is to identify the posterior distribution on  $\beta$

$$\mathbb{P}(\beta | \mathcal{D}_n) = \frac{\mathbb{P}(Y|X, \beta)\mathbb{P}(\beta)}{\mathbb{P}(Y|X)}. \quad (2)$$

If  $\mathbb{P}(\beta) = N(\beta; m_0, C_0)$ , then the posterior distribution  $\beta | \mathcal{D}_n \sim N(m_n, C_n)$  is given in closed form. Otherwise it is not.

Linear models of the form  $x^T \beta$  are quite flexible, once one considers basis function expansions. In other words,  $x = (1, \psi_0(s), \psi_1(s), \dots, \psi_p(s))$  for data  $s \in \mathbb{R}^d$  and some functions  $\{\psi_i\}$ , which can be a subset of polynomials [39, 22, 43], wavelets and other “ $x$ -lets” [21], radial basis functions [14], random feature models [69], or any number of other choices. The book [7] provides a concise and easy to read summary for regression applications. In fact, there are complete bases for many function-spaces. For example, if  $\Omega = [0, 1]^d$  then the Fourier series forms a complete basis for  $L^2(\Omega) = \{f : \Omega \rightarrow \mathbb{R}; \int_{\Omega} f(s)^2 ds < \infty\}$  [38] and a subset of such features can therefore be used to construct a convergent approximation. In fact, since shift-invariant kernel operators (those defined only in terms of differences,  $K(x, y) = k(x-y)$ ) are diagonalized by the Fourier basis, then the expectation of the product of two such features with an appropriately distributed random frequency is equal to the kernel evaluation. Monte Carlo approximation of such expectations is the basis of random feature models [69], which are another popular class of linear models in the machine learning literature.

An issue is how many terms to include, and perhaps more importantly, how to select a subset of the important terms from a sufficiently rich set, without incurring a loss in accuracy due to overfitting, as can occur with too much flexibility. The latter issue is often referred to as “variance-bias tradeoff”: a model which is too flexible (negligible bias) may be too strongly influenced by a particular data set, hence incurring a large variance over a range of different data sets [37]. This well-known issue can be dealt with by beginning with a sufficiently rich class of approximating functions (e.g. a large enough basis) and then introducing prior assumptions, or regularization, in order to let the model select the most parsimonious representation [82, 45, 81, 62, 61, 80].

## 1.2 Sparsity priors

In the context of prior selection, often the Gaussian assumption is considered too restrictive. In particular, it has become very popular at the end of the last and the beginning of this millenium to utilize a sparsity promoting prior. Motivated by sparsity penalties which have been successful in frequentist bridge regression [81, 21, 29] early sparsity priors simply replace the quadratic density associated to a Gaussian prior (ridge regression) with another density of the form  $\exp(-R(\beta))$ , where  $R(\beta) = |L\beta|_r^r$ , for  $r \in (0, 1]$ ,  $L : \mathbb{R}^{\bar{p}} \rightarrow \mathbb{R}^p$ , and  $|\beta|_r^r = \sum_{i=1}^{\bar{p}} |\beta_i|^r$  [68, 65, 3]. This can be extended to the case  $r = 0$ , which corresponds to counting measure on the non-zero elements  $|\beta|_0 = \sum_{i=1}^{\bar{p}} \mathbf{1}_{\{\beta_i \neq 0\}}$ . Note that if there is a  $W : \mathbb{R}^{\bar{p}} \rightarrow \mathbb{R}^{\bar{p}}$  such that  $WL = I_{\bar{p}}$ , then one can always redefine  $X_n \rightarrow X_n W$  and  $\beta \rightarrow L\beta$ . Therefore, we assume without loss of too much generality that  $L = I_p$ . This will be discussed further in the examples.

General sparsity-promoting priors of the type  $R(\beta) = f(|\beta|)$  are also possible, and this type of prior will be the focus of the present work, to be introduced in the following subsection. Collectively, this family of priors have come to be known as “shrinkage” priors because the resulting maximum a posteriori (MAP) estimator (or frequentist penalized maximum likelihood estimator (MLE)) tends to “shrink” all the coefficients towards zero. In particular, sufficiently small coefficients are exactly zero, which is the main impetus underlying their use, while the excess shrinkage leads to a non-desirable bias. In recent years “spike and slab” priors [58] have become very popular, as they soften this non-desirable property. Such priors are hierarchical, consisting of a mixture distribution with a Dirac mass at 0 (a spike) and a continuous distribution such as the ones considered here (a slab). See [5] for a recent review, focused on the spike and slab LASSO (SSLASSO).

There is a computational burden to performing inference with these more exotic priors, even in the case when we abandon uncertainty quantification (UQ) and settle for a MAP estimator. In the best case of  $R(\beta) = |\beta|_1$  we have a convex optimization problem, which can be solved efficiently by a number of modern methods, such as iterative soft thresholding [24, 13] and alternating direction method of multipliers [36, 12]. These methods are able to achieve a comparable cost to the solution of a least squares problem, i.e.  $\mathcal{O}(np)$  at best, and there is scope for per-iteration parallelization. However, there are limitations and drawbacks to this choice, and it is often desirable to promote sparsity more strongly, e.g. using non-convex  $R(\beta)$ , where there are no such default recipes [29]. The recently introduced SSLASSO [72] is a notable algorithm that delivers a point estimate which promotes sparsity more strongly than  $R(\beta) = |\beta|_1$  and at a comparable cost to the methods above.

Considering the full Bayesian posterior, the situation is even more daunting. Indeed once one adopts such a sparsity prior then the posterior is no longer characterized in closed form with finitely many parameters, as in the Gaussian case (in the finite/discrete/parametric case). Laplace approximation [7] requires derivative and Hessian of the log-posterior, which may not exist. Computationally-intensive methods such as Markov chain Monte Carlo (MCMC) [71] are required for consistent estimation, as proposed for the Bayesian LASSO (BL) in [65]. There has been a lot of activity in this direction in the past 10 years – see, e.g. [55, 57, 16, 85] for some examples from the applied mathematics and inverse problems communities and [66, 67, 9] for some examples from machine learning and statistics. Here we propose to employ a variational approach to recover the best Gaussian approximation to the sparsity-promoting posterior, in a sense to be defined precisely below. This approach provides approximate UQ for a substantially smaller cost than fully Bayesian approaches. Indeed the cost is only slightly larger than point estimation methods.

### 1.3 Contribution

The present work is focused on the case of Normal scale-mixtures of generalized inverse Gaussians (GIG), which will be referred to as Normal-GIG (N-GIG) priors. In particular, the prior of interest is the  $\beta$  marginal of the following hierarchical model

$$\mathbb{P}(\beta|\theta) = \prod_{j=1}^p N(\beta_j; 0, \theta_j), \quad \mathbb{P}(\theta) = \prod_{j=1}^p \mathcal{GIG}(\theta_j; \nu, \delta, \lambda), \quad (3)$$

where the distribution on  $\theta_j > 0$  is given by

$$\mathcal{GIG}(\theta_j; \nu, \delta, \lambda) \propto \theta_j^{\nu-1} \exp \left[ -\frac{1}{2}(\delta^2/\theta_j + \lambda^2\theta_j) \right]. \quad (4)$$

The  $GIG$  distribution is generalized above by defining it only as proportional to the right-hand side. One requires  $\nu > 0$  if  $\delta = 0$  and  $\nu < 0$  if  $\lambda = 0$  for a proper prior. Otherwise there are no constraints on the parameters. This family of priors was considered before in [75]. Some relevant examples which will be considered in the present work are: BL [2, 73], Jeffrey’s (Jeff) [34], Student-t (ST) [83], Normal-Gamma (NG) and Normal inverse Gaussian (NIG) [18, 42, 17]. See Figure 1 for an illustration and Table 1 for a summary of some relevant properties.

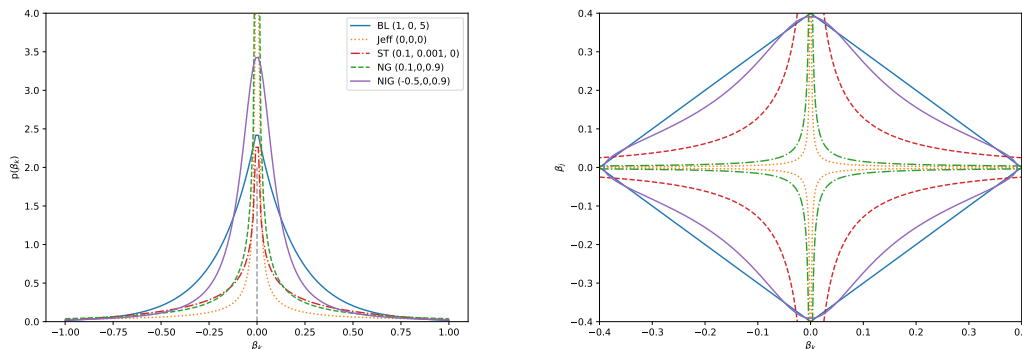


Figure 1: The left panel shows 1d density profiles for N-GIG priors on  $\beta_j$  considered in the present work. The right panel shows a contour for each example on a pair of covariates  $(\beta_j, \beta_k)$ . The range of permissible values of  $(\nu, \delta, \lambda)$ , as well as some properties of the examples, are given in Table 1. The particular values of  $(\nu, \delta, \lambda)$  in the plot are given in the legend of the left panel.

	BL	Jeff	ST	NG	NIG
$(\nu, \delta, \lambda)$	$(1, 0, \lambda)$	$(0, 0, 0)$	$(\nu < 1/2, \delta, 0)$	$(\nu, 0, \lambda)$	$(-1/2, \delta, \lambda)$
Singular at $\beta_j = 0$	No	Yes	No	Yes	No
Tail behavior	exponential	algebraic	algebraic	exponential	exponential

Table 1: N-GIG priors considered here and some relevant properties.

A variational Bayesian expectation maximization (VBEM) method [6, 4] will be employed for approximation of the resulting posterior, which requires only the solution of (unconstrained) linear systems, and provides approximations of the mean and covariance of the target. Additionally, in parallel we will perform classical expectation maximization (EM) [27] to obtain the maximum a posteriori (MAP) estimator. This approach will deliver the *variational Bayesian LASSO* (VBL), a principled Gaussian approximation to the BL, as well as variational approximation associated to the other N-GIG priors listed in Table 1.

In the Bayesian community, recent theoretical results have revealed that the BL is suboptimal in both parameter estimation and variable selection [20]. However [77] have shown that many shrinkage priors are consistent. The necessary condition is that the tail should decay algebraically and not exponentially, which includes ST and Jeff above. Also, it is well-known that the mean of sparsity priors, such as the total variation (TV) prior, may not promote sparsity [53]. In fact, in this work it is shown that in the limit of  $p \rightarrow \infty$ , for different choices of  $\lambda$  depending on  $p$ , the posterior associated to a TV prior is either a Gaussian or has a diverging mean. Indeed even the BL point estimator [65], which returns the median instead of the mean, is not as sparse as the standard LASSO, i.e. its MAP estimator. Despite these shortcomings, VBL is still considered

here as a prominent example, due to the persistent ubiquity of (B)LASSO as a model of choice across science and engineering applications.

VBEM is a particular instance of a more general methodology known as *mean-field variational Bayes*. See [10] for a recent review. The ST example is referred to as automatic relevance detection [62, 56], and variational inference for this model has been introduced, independently, in [8] and [31]. The work [3] considers variational inference in the context of the stable mixing distribution on  $\theta$  in (3). The distribution cannot be explicitly represented in general, but yields a nice family of marginal priors of the form  $\propto \exp(-\lambda|\beta|_r^r)$  for  $r \in (0, 2)$ , which is referred to as Bayesian bridge regression, and includes BL. It is important to note that such variational mean-field models are only an approximation of the original full Bayesian model, and as such the UQ delivered is not precise – see e.g. [63] for a careful study of some related models in this context.

The approach presented here provides fast UQ in the context of sparse regression and linear inverse problems. The key points are:

- Fast and inexpensive variational Bayesian solution with **sparsity** promoting priors. The Bayesian formulation provides **UQ** in the estimate, which is becoming increasingly important in science and engineering applications [76, 39].
- **Online** variational Bayesian solution means arbitrarily large  $n$  can be handled with a  $\mathcal{O}(p^2)$  memory cost and  $\mathcal{O}(p^3)$  compute cost per update, where  $p$  is the width of the design matrix (see below). The method provides **exact** MAP estimate (for convex prior) and *variational approximation to the posterior*, with little more than a pair of parallel Kalman filters [49]. We note that the results presented are constrained to the case of regression, but will be extended to classification and non-trivial dynamics in future work.
- **Adaptive** online learning of hyper-parameters via EM approach provides improved accuracy at a marginal additional cost.
- A further “low rank + diagonal” **approximation** provides a reduction in cost to  $\mathcal{O}(p)$  in case  $p$  is prohibitively large, in a similar spirit to the ensemble Kalman filter (EnKF) [33].

The rest of the paper is organized as follows. The basic model is introduced in Section 2: after introducing the basic model in Section 2.1, Section 2.2 describes MAP estimation with the EM algorithm, and Section 2.3.1 describes posterior approximation using VBEM, culminating in our Gaussian approximation of sparsity-promoting posteriors and VBL in Section 2.3.2. Further enhancements to the basic model are introduced in Section 3. In particular, the online version is introduced in Section 3.1, and hyper-parameter tuning is considered in Section 3.2. Numerical results are presented in Section 4, including a small basic dataset relating to diabetes in Section 4.1, a comparison-study with state-of-the-art competitors on a prototype problem used before to evaluate variable selection capability in Section 4.2, and more computationally intensive (generalized) total variation (TV) denoising/deblurring examples in Section 4.3.

## 2 The basic model and method

### 2.1 The model: a Bayesian formulation of sparsity priors

The basic model considered here is given by (1), (3), and (4), iterated compactly here for clarity

$$\begin{aligned} Y_n | X_n, \beta &\sim N(X_n \beta, \gamma^2 I_n), \\ \beta | \theta &\sim N(0, D(\theta)), \quad D(\theta) := \text{diag}(\theta_1, \dots, \theta_p), \\ \theta_j &\sim \mathcal{GIG}(\theta_j; \nu, \delta, \lambda), \text{ i.i.d. for } j = 1, \dots, p. \end{aligned} \quad (5)$$

The conditionals of the joint are known exactly

$$\beta | \theta, X_n, Y_n \sim \mathcal{N}(\beta; m_n^\theta, C_n^\theta), \quad (6)$$

$$\theta_j | \beta, X_n, Y_n \sim \mathcal{GIG}(\theta_j; \nu - 1/2, \sqrt{\delta^2 + \beta_j^2}, \lambda), \quad (7)$$

where  $m_n^\theta, C_n^\theta$  are given by [11]

$$\begin{aligned} m_n^\theta &= (X_n^T X_n + \gamma^2 D(1/\theta))^{-1} X_n^T Y_n \\ &= D(\theta) X_n^T (\gamma^2 I_n + X_n D(\theta) X_n^T)^{-1} Y_n, \end{aligned} \quad (8)$$

$$\begin{aligned} C_n^\theta &= \left( \frac{1}{\gamma^2} X_n^T X_n + D(1/\theta) \right)^{-1} \\ &= \left( I_p - D(\theta) X_n^T (\gamma^2 I_n + X_n D(\theta) X_n^T)^{-1} X_n \right) D(\theta). \end{aligned} \quad (9)$$

By choosing the appropriate version above, the computation cost is  $\mathcal{O}(pn \min\{p, n\})$ , and the memory cost is  $\mathcal{O}(pn)$ . In case  $n > p$ , and in particular if  $n \rightarrow \infty$ , then the Kalman filter [49] provides exact solution online with a memory and (per iteration) computation cost of  $\mathcal{O}(p^2)$ . See Appendix C.

Since the conditionals are known, Gibbs sampling can be used to sample exactly from the posterior [75, 65]. Sequential Monte Carlo methods [30, 59] have also been designed to sample from the full posterior sequentially in [75, 17], and a sequential expectation maximization (EM) [27] method has been used to approximate MAP estimates of  $\beta | (X_n, Y_n)$  in [18, 17].

**Example 2.1** Assume that the prior consists of  $p$  independent random variables  $\beta_j$ , each with Laplace distribution  $\mathcal{L}(\beta_j; \lambda)$ , the BL model. The MAP estimator associated to this model corresponds to  $L1$  regularized regression, or LASSO [81]. It is well-known that the Laplace distribution can be expressed as a scale mixture of GIG with parameters  $(1, 0, \lambda)$ :

$$\mathcal{L}(\beta_j; \lambda) = \int_{\mathbb{R}_+} \mathcal{N}(\beta_j; 0, \theta_j) \mathcal{GIG}(\theta_j; 1, 0, \lambda) d\theta_j. \quad (10)$$

**Remark 2.1** If (5) is modified as  $\mathbb{P}(\beta | \theta) = \mathcal{N}(\beta; 0, (C_0^{-1} + D(1/\theta))^{-1})$  and one replaces  $D(1/\theta) \leftarrow C_0^{-1} + D(1/\theta)$  in (8) and (9), then marginally one has an elastic net prior for  $\delta = 0$  and  $\nu = 1$ :  $\mathbb{P}(\beta) \propto \mathcal{N}(\beta; 0, C_0) \mathcal{L}(\beta; \lambda)$  [73].

### 2.2 MAP estimation by Expectation maximization

For the next sections we suppress  $X$  and  $n$  in the notation where convenient. Suppose we want to maximize

$$\log \mathbb{P}(Y, \beta) = \log \int \mathbb{P}(Y, \beta, \theta) d\theta \geq \int \log \left( \frac{\mathbb{P}(Y, \beta, \theta)}{q(\theta)} \right) q(\theta) d\theta, \quad (11)$$

where the inequality arises (for *any* probability density  $q(\theta) > 0$ ) from an application of Jensen's inequality, and  $\mathbb{P}$  here denotes a probability density. The expectation maximization (EM) algorithm [27] proceeds as follows. Define  $q^t(\theta) = \mathbb{P}(\theta|\beta^t, Y)$ ,

$$Q(\beta|\beta^t) = \int \log \left( \frac{\mathbb{P}(Y, \beta, \theta)}{\mathbb{P}(\theta|\beta^t, Y)} \right) \mathbb{P}(\theta|\beta^t, Y) d\theta, \quad (12)$$

and let  $\beta^{t+1} = \operatorname{argmax}_{\beta} Q(\beta|\beta^t)$ .

In our context this entails iteratively computing

$$Q(\beta|\beta^t) = \frac{1}{2} \beta^T D(1/\theta^{t+1}) \beta + \frac{1}{2\gamma^2} |Y_n - X_n \beta|_2^2 + \kappa(\beta^t, X_n, Y_n) \quad (13)$$

where we recall that  $D(1/\theta^{t+1})$  is the diagonal matrix with  $1/\theta_j^{t+1}$  on the diagonal, and  $\kappa(\beta^t, X_n, Y_n)$  is a constant depending on  $\beta^t, X_n, Y_n$  but not  $\beta$ . For example, in the case of  $\delta \geq 0$  and  $\nu = 1$ ,  $\theta^{t+1}$  is defined element-wise as

$$1/\theta_j^{t+1} := \mathbb{E} [1/\theta_j | \beta^t, X_n, Y_n] = \lambda((\beta_j^t)^2 + \delta^2)^{-1/2}. \quad (14)$$

The calculation of (13) is given in Appendix A along with a slightly lengthier explanation of EM. Note we have assumed  $\nu = 1$  but allowed  $\delta \neq 0$  in the hyperprior (4), which relaxes the marginal Laplace identity (10). The general form of (14) is given in equation (38), and the case  $\nu = 0$  is given in (40). For  $\nu = 1$ , one then has the iteration

$$\mu_n^{t+1} = \left( X_n^T X_n + \gamma^2 \lambda D \left( ((\mu_n^t)^2 + \delta^2)^{-1/2} \right) \right)^{-1} X_n^T Y_n. \quad (15)$$

These analytical calculations have been shown and used before in several works, including [34, 18, 42]. From this, one obtains the MAP estimator at convergence  $\mu_n^t \rightarrow \mu_n$ .

**Remark 2.2** *An iteratively reweighted least squares (IRLS) algorithm [46] can be derived in order to approximate regularization with  $r \in (0, 1]$  by a sequence of problems with  $r = 2$ , based on the following observation*

$$|\beta|_r^r = \sum_{i=1}^p |\beta_i|^r = \sum_{i=1}^r |\beta_i|^{r-2} \beta_i^2.$$

*The resulting iteration for  $r = 1$  is exactly as in (15), where  $\delta^2 > 0$  is interpreted as a regularization parameter. It can be shown under appropriate assumptions that  $\mu_n^t \rightarrow \mu_n$  as  $t \rightarrow \infty$ , where  $\mu_n$  is sparse if such solution exists, and convergence is linear (exponentially fast) for  $\mu_n^t$  sufficiently close to  $\mu_n$  [25].*

## 2.3 Posterior approximation

### 2.3.1 Variational Bayesian Expectation maximization

Here we propose to use the variational Bayesian expectation maximization (VBEM) algorithm, introduced in the context of graphical models in [4, 6]. We show how it works elegantly in our context to provide a Gaussian approximation to problems with sparsity priors, which is optimal in a certain sense. Suppose we return to (11), and this time multiply/divide by some density  $q(\beta) > 0$  and integrate over  $\beta$  as well. Then we have the evidence lower bound

$$\log \mathbb{P}(Y) = \log \int \mathbb{P}(Y, \beta, \theta) d\theta d\beta \geq \int \log \left( \frac{\mathbb{P}(Y, \beta, \theta)}{q(\theta)q(\beta)} \right) q(\theta)q(\beta) d\theta d\beta. \quad (16)$$



Coincidentally, maximizing this with respect to the *densities*  $q(\theta)q(\beta)$  coincides with minimizing the KL divergence between this variational approximation and the joint posterior, i.e.

$$\begin{aligned} \log \mathbb{P}(Y) - \int \log \left( \frac{\mathbb{P}(Y, \beta, \theta)}{q(\theta)q(\beta)} \right) q(\theta)q(\beta) d\theta d\beta &= - \int \log \left( \frac{\mathbb{P}(\beta, \theta|Y)}{q(\theta)q(\beta)} \right) q(\theta)q(\beta) d\theta d\beta \\ &=: KL [q(\theta)q(\beta) || \mathbb{P}(\beta, \theta|Y)]. \end{aligned} \quad (17)$$

The objective functions for each of  $q(\theta)$  and  $q(\beta)$  given the other are convex and can be minimized exactly, as observed in [4, 6], leading to the iterative algorithm

$$\begin{aligned} q^{t+1}(\theta) &\propto \exp \left( \int \log \mathbb{P}(Y, \beta, \theta) q^t(\beta) d\beta \right), \\ q^{t+1}(\beta) &\propto \exp \left( \int \log \mathbb{P}(Y, \beta, \theta) q^{t+1}(\theta) d\theta \right). \end{aligned} \quad (18)$$

Furthermore, following from convexity of the intermediate targets this gives a descent direction for (17)  $KL [q^{t+1}(\theta)q^{t+1}(\beta) || \mathbb{P}(\beta, \theta|Y)] \leq KL [q^t(\theta)q^t(\beta) || \mathbb{P}(\beta, \theta|Y)]$ . Observe that constraining to  $q^{t+1}(\beta) = \delta_{\beta^{t+1}}(\beta)$ , where  $\delta(\cdot)$  is the Dirac delta function and  $\beta^{t+1}$  is the point of maximum probability above, yields the original EM algorithm. Also, observe that (18) may itself be intractable in general, although it is shown in [6] that it is simplified somewhat for conjugate exponential models and may be analytically soluble. Fortunately, the present situation is the best case, where it is analytically soluble. Notice that the objective function (17) corresponds to an independence assumption between  $\theta$  and  $\beta$ , however from (18) it is clear that the solution solves a coupled system, and in fact *probabilistic dependence is replaced with a deterministic dependence on each others' summary statistics*, as noted in [6].

### 2.3.2 Gaussian approximation to a sparsity promoting posterior

We approximate the model in (5) using the variational Bayesian approach of Section 2.3.1. Equations (18) are given by

$$\begin{aligned} q^{t+1}(\theta) &\propto \exp \left( -\frac{1}{2} \sum_{j=1}^p \mathbb{E}_t[\beta_j^2] / \theta_j \right) \mathbb{P}(\theta | \lambda), \\ q^{t+1}(\beta) &\propto \exp \left( -\frac{1}{2} \sum_{j=1}^p \beta_j^2 \mathbb{E}_{t+1}[1/\theta_j] - \frac{1}{2\gamma^2} |Y_n - X_n \beta|_2^2 \right), \end{aligned} \quad (19)$$

where  $\mathbb{E}_t$  is used to (degenerately) denote expectation with respect to the iteration  $t$  intermediate variational distribution, with respect to its argument,  $\beta$  or  $\theta$ . This is referred to as *coordinate ascent variational inference* [10]. The first equation looks similar to the EM algorithm, however with the important difference

$$q^{t+1}(\theta_j) = \mathcal{GIG} \left( \theta_j; \nu - 1/2, \sqrt{\delta^2 + C_{n,jj}^t + (m_{n,j}^t)^2}, \lambda \right), \quad (20)$$

where  $(m_n^t, C_n^t)$  are the mean and covariance of  $q^t(\beta) = N(\beta; m_n^t, C_n^t)$  (note the appearance of the variance  $C_{n,jj}^t$  instead of just  $(m_{n,j}^t)^2$ ).

This means that for the case  $\nu = 1$  we have

$$1/\theta_{n,j}^{t+1} := \mathbb{E}_{t+1}[1/\theta_j] = \lambda(C_{n,jj}^t + (m_{n,j}^t)^2 + \delta^2)^{-1/2}. \quad (21)$$



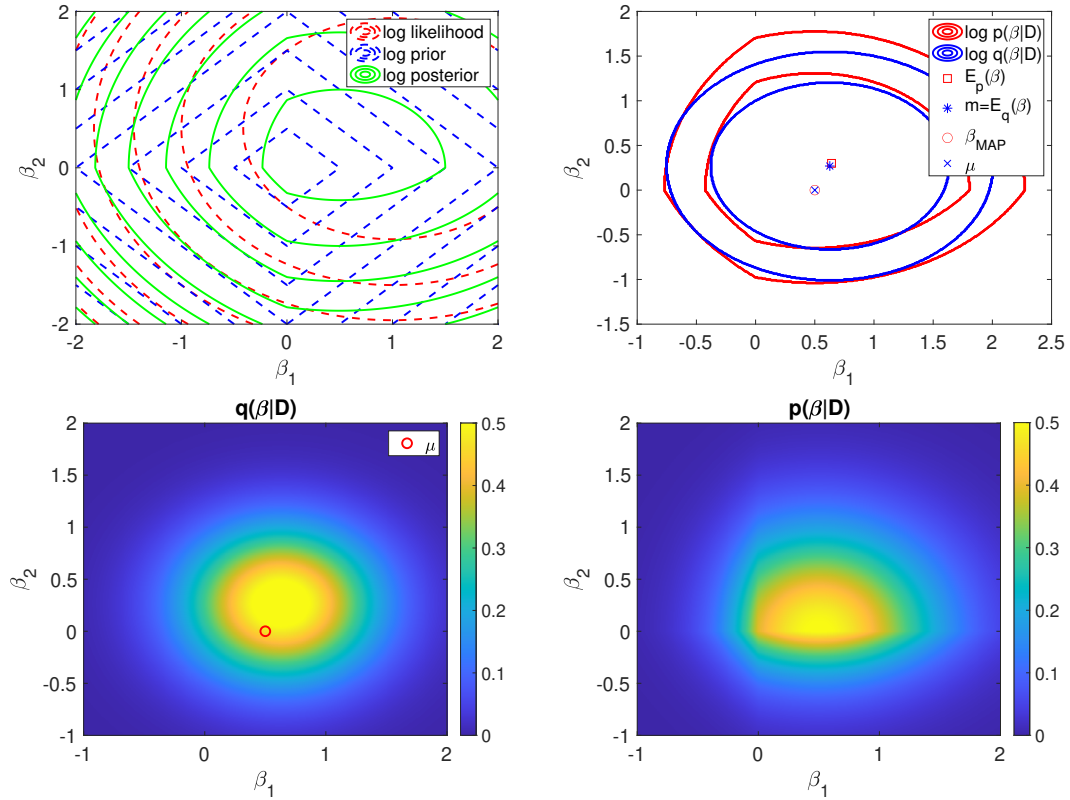


Figure 2: Illustration of the variational Bayesian LASSO (VBL). The top left figure shows the contours of the prior, the likelihood, and the posterior. The top right figure shows the  $\alpha = 0.8$  and  $\alpha = 0.95$  HPD credible contours of the posterior  $\mathbb{P}(\beta|\mathcal{D})$  and the variational approximation  $q(\beta|\mathcal{D})$ , along with means and MAPs. For this example, the posterior median is very close to the mean, but slightly towards the MAP. The bottom row shows the density of VBL (left, with MAP estimate  $\mu$ ) and the posterior (right).

The update equations are given by

$$m_n^{t+1} = C_n^{t+1} \left( \frac{1}{\gamma^2} X_n^T Y_n \right), \quad (22)$$

$$C_n^{t+1} = \left( \frac{1}{\gamma^2} X_n^T X_n + D(1/\theta_n^{t+1}) \right)^{-1}. \quad (23)$$

Here we can explicitly observe the deterministic dependence between the marginally optimal  $\theta$  and  $\beta$  distributions via each others' summary statistics. The general form of the update (21) is given in (38), and the case  $\nu = 0$  is given in (40).

Note that this algorithm runs for approximately the same cost as the former, and provides a Gaussian approximation  $(m_n^*, C_n^*)$  of the posterior. The former provides an approximation of the MAP estimator  $\mu_n^*$ . In the case  $\nu = 1$  we refer to this triple  $(\mu_n^*, m_n^*, C_n^*)$  as the variational Bayesian LASSO (VBL). This is summarized in Algorithm 1. In the context of UQ, one may consider the sparse solution to be reasonable if, for any index  $j$  such that  $\mu_{n,j} = 0$ , one has  $0 \in (m_{n,j} - 2\sqrt{C_{n,jj}}, m_{n,j} + 2\sqrt{C_{n,jj}})$ , i.e. the origin is within the credible interval of the variational Bayesian marginal for those coordinates which are predicted to vanish. In general, one may flag as unusual any circumstances where  $\mu_{n,j} \notin (m_{n,j} - 2\sqrt{C_{n,jj}}, m_{n,j} + 2\sqrt{C_{n,jj}})$ . See Figure 2 for an illustration of the VBL applied to a simple example with  $p = n = 2$  ("exact" values are calculated with numerical quadrature on the domain  $[-4, 4]^2$  with 1000 grid points in each direction). The  $\alpha$  highest posterior density (HPD) credible contour of a density  $\mathbb{P}$  is defined by  $\{\beta; \mathbb{P}(\beta) = c(\alpha)\}$ , where  $c(\alpha)$  solves

$$\int_{\{\beta; \mathbb{P}(\beta) \geq c(\alpha)\}} \mathbb{P}(\beta) d\beta = \alpha.$$

The top right panel shows the  $\alpha$  HPD credible contours of  $\mathbb{P}(\beta|\mathcal{D}_n)$  and  $q(\beta|\mathcal{D}_n)$  associated to  $\alpha = 0.8$  and  $\alpha = 0.95$ .

**Remark 2.3** *Step (3) of Algorithm 1 requires a stopping criterion. A good, if somewhat cumbersome, option is  $d((\mu^t, m^t, C^t), (\mu^{t-1}, m^{t-1}, C^{t-1})) = |\text{ELBO}_t - \text{ELBO}_{t-1}|/|\text{ELBO}_t|$ , where  $\text{ELBO}_t$  is the lower bound appearing on the right-hand side of (16), which can be computed in closed form. Another simpler option is  $d((\mu^t, m^t, C^t), (\mu^{t-1}, m^{t-1}, C^{t-1})) = \|Xm^t - Y\|/\gamma$ . We will see that the algorithm returns a good estimator very quickly, but may take a long time to converge, and may even return a worse estimator at convergence. Therefore, a maximum number of iterations is often also employed as an alternative in practice.*

### 3 Enhanced model

This section focuses on enhancing the model by enabling sequential/online inference and hyperparameter optimization. The static version, with fixed  $n$ , given in (8) and (9) will henceforth be referred to as *monolithic* so that the distinction is clear.

#### 3.1 Online Gaussian approximation to a sparsity posterior

In the following we focus the description on  $(m_n, C_n)$  of the VBEM formulation (22), (23), but note that analogous equations hold for  $\mu_n$  (15). There are two distinct scenarios to consider here. First we will consider the case of moderate  $p$  and  $n \gg p$ , where the online method reproduces EM and VBEM exactly at a cost of  $\mathcal{O}(p^3)$  per iteration. The second case we will consider is that of very large  $p$ , and possibly  $n \leq p$ , where it is necessary to impose an approximation in order to control the cost by  $\mathcal{O}(p)$ . Both approaches are amenable to online implementation, i.e.  $n \rightarrow \infty$ .

---

**Algorithm 1** Variational Bayesian N-GIG.

---

**Input:** Design matrix  $X$ , labels  $Y$ , parameters  $\gamma, \lambda, \delta, \nu$ , initial guess  $(\mu^0, m^0, C^0) \in \mathbb{R}^{2p+p^2}$ , convergence criteria  $\epsilon, T > 0$  and distance function  $d: \mathbb{R}^{(2p+p^2) \times (2p+p^2)} \rightarrow \mathbb{R}_+$ .

1. Specify functional forms  $\theta_{\text{VBEM}}^{t+1}(\beta)$  and  $\theta_{\text{EM}}^{t+1}(\beta)$  based on  $\delta, \nu$ , as given in (38).
2. Set  $t = 0$ , and  $(\mu^{-1}, m^{-1}, C^{-1}) = \mathbf{0}_{2p+p^2}$  (all zeros).
3. **While**  $t \leq T$  **and**  $d((\mu^t, m^t, C^t), (\mu^{t-1}, m^{t-1}, C^{t-1})) > \epsilon$ ;
  - (a) Compute  $\theta_{\text{VBEM}}^{t+1}$  and  $\theta_{\text{EM}}^{t+1}$  (arguments suppressed);
  - (b) Compute

$$G_{\text{VBEM}}^{t+1} = D(\theta_{\text{VBEM}}^{t+1})X^T(XD(\theta_{\text{VBEM}}^{t+1})X^T + \gamma^2 I_n)^{-1}, \quad (24)$$

$$G_{\text{EM}}^{t+1} = D(\theta_{\text{EM}}^{t+1})X^T(XD(\theta_{\text{EM}}^{t+1})X^T + \gamma^2 I_n)^{-1}. \quad (25)$$

- (c) Compute

$$m^{t+1} = G_{\text{VBEM}}^{t+1}Y, \quad (26)$$

$$C^{t+1} = (I - G_{\text{VBEM}}^{t+1}X)D(\theta_{\text{VBEM}}^{t+1}), \quad (27)$$

$$\mu^{t+1} = G_{\text{EM}}^{t+1}Y. \quad (28)$$

- (d)  $t=t+1$ .

**Output:**  $(\mu^*, m^*, C^*) \in \mathbb{R}^{2p+p^2}$ .

---

### 3.1.1 Small/moderate $p$ exact method

Suppose we are assimilating batches of size  $M$ , and denote

$$\bar{X}_n = X_{nM}, \quad \bar{Y}_n = Y_{nM}, \quad \tilde{X}_n = [x_{(n-1)M+1}, \dots, x_{nM}]^T, \quad \tilde{Y}_n = [y_{(n-1)M+1}, \dots, y_{nM}]^T,$$

so that e.g.  $\tilde{X}_n^T \tilde{X}_n = \sum_{i=(n-1)M+1}^{nM} x_i x_i^T$ . Sequential batches are presented but this may not always be a sensible choice and some permutation of the indices may make sense. See Remark 3.2. We can compute batch updates of the required matrices in (8) exactly with a total of at most  $\mathcal{O}(p^2 M)$  operations:

$$\bar{X}_n^T \bar{X}_n = \bar{X}_{n-1}^T \bar{X}_{n-1} + \tilde{X}_n^T \tilde{X}_n, \quad \bar{X}_n^T \bar{Y}_n = \bar{X}_{n-1}^T \bar{Y}_{n-1} + \tilde{X}_n^T \tilde{Y}_n, \quad \bar{Y}_n^T \bar{Y}_n = \bar{Y}_{n-1}^T \bar{Y}_{n-1} + \tilde{Y}_n^T \tilde{Y}_n.$$

The cost may be smaller if the intermediate quantities are sparse (many zeros) or low-rank. We have the following equation for the precision  $(C_n^t)^{-1} = \frac{1}{\gamma^2} \bar{X}_n^T \bar{X}_n + D(1/\theta_n^t)$  and can proceed directly with iterating (22) and (23). In the worst case scenario, the inversion required to compute (22) will incur a cost of  $\mathcal{O}(p^3)$ , so one would aim to take  $M = p$ . We iterate that the focus here is the case  $n \gg p$ . For large  $p$ , which will be discussed now,  $\bar{X}_n^T \bar{X}_n$  must be sparse or low-rank. In this case, inversion can be done approximately with a cost of as little as  $\mathcal{O}(p)$ . In case  $\mathcal{O}(p^2)$  is prohibitive for computation or memory, then online computation and storage of the component matrices must be controlled as well. This is discussed further in the following section.

### 3.1.2 Large $p$ approximate method

In the case of large  $p$  and/or  $n \leq p$ , the problem is different. It is preferable to directly confront the monolithic problem (8) if it is possible, for example in case that  $n < \infty$  is fixed and  $X_n$  is sufficiently sparse and/or low-rank to allow the direct use of an iterative Krylov-type solver [44, 74]. On the other hand, if this cannot be handled directly, then a sequential/online strategy can be adopted as follows.

It is first instructive to observe the following recursive formulation of (8)

$$\begin{aligned} m_n &= \left( \frac{1}{\gamma^2} \bar{X}_n^T \bar{X}_n + D(1/\theta) \right)^{-1} \left( \frac{1}{\gamma^2} (\tilde{X}_n^T \tilde{Y}_n + \bar{X}_{n-1}^T \bar{X}_{n-1} m_{n-1}) + D(1/\theta) m_{n-1} \right) \\ &= m_{n-1} + D(\theta) \bar{X}_n^T (\gamma^2 I_n + \bar{X}_n D(\theta) \bar{X}_n^T)^{-1} (\hat{Y}_n - \bar{X}_n m_{n-1}), \end{aligned} \quad (29)$$

where  $\hat{Y}_n := ((\bar{X}_{n-1} m_{n-1})^T, \tilde{Y}_n^T)^T$ . This observation is obviously not useful by itself, as it incurs a cost of  $\mathcal{O}(\min\{p, n\}^3)$  per iteration, whereas the Kalman filter delivers  $\mathcal{O}(p^2)$  updates in primal/covariance form (see (50)). However, the precision  $\bar{X}_n^T \bar{X}_n + D(1/\theta)$  is required for our VBEM method in order to update  $\theta$ . The representation above facilitates a recursive ‘‘rank  $M$  + diagonal’’ approximation in similar spirit to the ensemble Kalman filter [15], which allows us to effectively pass information forward in an online fashion.

In particular, suppose we have  $\hat{X}_{n-1} \in \mathbb{R}^{M \times p}$  s.t.  $\bar{X}_{n-1}^T \bar{X}_{n-1} \approx \hat{X}_{n-1}^T \hat{X}_{n-1}$ , so that

$$(C_{n-1}^*)^{-1} \approx \frac{1}{\gamma^2} \hat{X}_{n-1}^T \hat{X}_{n-1} + D(1/\theta_{n-1}^*).$$

Now, recall equation (29) and define

$$\hat{Y}_n := \begin{pmatrix} \hat{X}_{n-1}^T m_{n-1} \\ \tilde{Y}_n \end{pmatrix} \in \mathbb{R}^{2M}, \quad \mathbf{X}_n := \begin{pmatrix} \hat{X}_{n-1} \\ \tilde{X}_n \end{pmatrix} \in \mathbb{R}^{2M \times p}.$$

The  $\mathcal{O}(2Mp)$  update which replaces (22) and (23) is given by

$$m_n^{t+1} = m_{n-1} + D(\theta_n^{t+1})\mathbf{X}_n^T (\gamma^2 I_{2M} + \mathbf{X}_n D(\theta_n^{t+1})\mathbf{X}_n^T)^{-1} (\hat{Y}_n - \mathbf{X}_n m_{n-1}), \quad (30)$$

$$C_n^{t+1} = \left( I_p - D(\theta_n^{t+1})\mathbf{X}_n^T (\gamma^2 I_{2M} + \mathbf{X}_n D(\theta_n^{t+1})\mathbf{X}_n^T)^{-1} \mathbf{X}_n \right) D(\theta_n^{t+1}). \quad (31)$$

Finally we need  $\hat{X}_n \in \mathbb{R}^{M \times p}$  s.t.  $\hat{X}_n^T \hat{X}_n \approx \mathbf{X}_n^T \mathbf{X}_n$  in order to proceed to the next iteration. This is achieved by (i) computing a reduced rank- $M$  eigendecomposition  $\mathbf{X}_n \mathbf{X}_n^T \approx U \Sigma^2 U^T$ , with  $\Sigma \in \mathbb{R}^{M \times M}$  diagonal and  $U \in \mathbb{R}^{2M \times M}$  orthogonal, and (ii) defining  $\hat{X}_n := U^T \mathbf{X}_n$ . This approximation in principle costs  $\mathcal{O}(4M^2(p+2M))$  but with a memory cost of only  $\mathcal{O}(Mp)$ . All the steps above are summarized in Algorithm 2. It is clear that in terms of cost one wants to choose  $M$  small, but in terms of accuracy one wants to choose  $M$  large, so these considerations should be balanced.

**Remark 3.1 (EnKF)** *We note the similarity between the above procedure and a (square-root) EnKF [54] for solution of (50) and (51), which proceeds with a low-rank (or low-rank plus diagonal) approximation of the covariance  $C_n$ . In our scenario, the above framework is more natural and is expected to provide a better approximation. It may also be useful for quadratic/Tikhonov regularization where  $\theta$  is held constant, as an “EnKF for regression”, since it delivers a natural non-degenerate covariance approximation. This is described further in Appendix C.*

**Remark 3.2 (Batching strategy)** *In the offline scenario where the data size  $n > 0$  is fixed and the sequential method is employed then choice of batches is important. If the inputs are i.i.d. random samples then sequential batching is sensible, i.e.  $(1, 2, \dots, M)$ ,  $(M+1, \dots, 2M)$ , etc. Otherwise if there is structure in the inputs (e.g. in the context of inverse problems) then it makes more sense to use random sampling without replacement or evenly spread out batches  $(1, 1+b, 1+2b, \dots, n)$ ,  $(2, 2+b, 2+2b, \dots, n)$ , etc., where  $b = n/M$ .*

### 3.1.3 Further discussion

Note that in practice one would hope that after some iterations  $(\mu_n, m_n, C_n)$  will not be changing very much with the iterative re-weighting, and few inner updates will be required, if any. If the model is stationary, then one may also not need to allow  $n \rightarrow \infty$ . There are some other modifications which could be made along the way to further improve efficiency, such as thresholding, i.e.  $m_n \rightarrow \mathbf{1}_{\{\epsilon < |m_n|\}} m_n$ , for small  $\epsilon > 0$ , where  $\mathbf{1}_A$  is the indicator function on the set  $A$ , and it acts elementwise on the entries of  $m_n$  (and similar for  $\mu_n$ ). Suppose that  $m_n$  has essentially converged, and  $p' \ll p$  parameters are non-zero. We can then discard the 0-valued parameters, thereby either vastly speeding up the algorithm or making way for inclusion of  $p - p'$  new parameters. Similar things have been done before. See e.g. [86] and [3]. In the latter article it is noted that this also mitigates a problem with singularity, which is not an issue here because we use the dual formulation of the problem – see (24), (26).

All of the present technology is well-suited to an online scenario, where one assumes a fixed static problem but data arrives sequentially in time, and may continue indefinitely (i.e.  $n \rightarrow \infty$ ). If this model is meant to emulate a computer simulation, for example which is called by another computer simulation for a particular value of inputs, as in the common case of coupled multi-physics systems and whole device modelling, then one can decide whether the emulator is suitable for a given query input, for example by evaluating the uncertainty under the current approximation  $x(s)^T C_n x(s)$ . If this is below a certain level then the model returns  $m_n^T x(s)$  (and possibly also  $x(s)^T C_n x(s)$  if the requesting program is capable of handling uncertainty), otherwise the emulator requests a label from the computer simulation and is updated accordingly,

---

**Algorithm 2** Online Approximate Variational Bayesian N-GIG (large  $p$ ).

---

**Input:** Design matrix  $X$ , labels  $Y$  (possibly infinite and arriving online), parameters  $\gamma, \lambda, \delta, \nu$ , initial guess  $(\mu^0, m^0, C^0) \in \mathbb{R}^{2p+p^2}$ , inner convergence criteria  $\epsilon, T > 0$ , distance function  $d : \mathbb{R}^{(2p+p^2) \times (2p+p^2)} \rightarrow \mathbb{R}_+$ , batch size  $M$  and rule for batching (see Remark 3.2).

1. Set  $n = 1$ ,  $\hat{X}_1 = X_1$ . **Do** Algorithm 1, and output  $(\mu_1^*, m_1^*, C_1^*)$  and functional forms  $\theta_{\text{VBEM}}^{t+1}(\beta)$  and  $\theta_{\text{EM}}^{t+1}(\beta)$ , as given in (38).

2. For  $n = 2, \dots$

(a) Set  $t = 0$ ,  $(\mu_n^0, m_n^0, C_n^0) = (\mu_{n-1}^*, m_{n-1}^*, C_{n-1}^*)$ ,  $(\mu_n^{-1}, m_n^{-1}, C_n^{-1}) = \mathbf{0}_{2p+p^2}$ ,

$$\hat{Y}_n^{\text{VBEM}} = \begin{pmatrix} \hat{X}_{n-1} m_{n-1}^* \\ \tilde{Y}_n \end{pmatrix}, \quad \hat{Y}_n^{\text{EM}} = \begin{pmatrix} \hat{X}_{n-1} \mu_{n-1}^* \\ \tilde{Y}_n \end{pmatrix}, \quad X_n = \begin{pmatrix} \hat{X}_{n-1} \\ \tilde{X}_n \end{pmatrix}.$$

(b) **While**  $t \leq T$  and  $d((\mu_n^t, m_n^t, C_n^t), (\mu_n^{t-1}, m_n^{t-1}, C_n^{t-1})) > \epsilon$ ;

i. Compute  $\theta_{\text{VBEM}}^{t+1}$  and  $\theta_{\text{EM}}^{t+1}$  (arguments suppressed);

ii. Compute

$$\mathbf{G}_{\text{VBEM}}^{t+1} = D(\theta_{\text{VBEM}}^{t+1}) X_n^T (X_n D(\theta_{\text{VBEM}}^{t+1}) X_n^T + \gamma^2 I_{2M})^{-1}, \quad (32)$$

$$\mathbf{G}_{\text{EM}}^{t+1} = D(\theta_{\text{EM}}^{t+1}) X_n^T (X_n D(\theta_{\text{EM}}^{t+1}) X_n^T + \gamma^2 I_{2M})^{-1}. \quad (33)$$

iii. Compute

$$m_n^{t+1} = m_{n-1}^* + \mathbf{G}_{\text{VBEM}}^{t+1} (\hat{Y}_n^{\text{VBEM}} - X_n m_{n-1}^*), \quad (34)$$

$$C_n^{t+1} = (I_p - \mathbf{G}_{\text{VBEM}}^{t+1} X_n) D(\theta_{\text{VBEM}}^{t+1}), \quad (35)$$

$$\mu_n^{t+1} = \mu_{n-1}^* + \mathbf{G}_{\text{EM}}^{t+1} (\hat{Y}_n^{\text{EM}} - X_n \mu_{n-1}^*). \quad (36)$$

iv.  $t=t+1$ .

(c) Compute rank  $M$  approximation  $U \Sigma^2 U^T \approx X_n X_n^T$ , and set  $\hat{X}_n := U^T X_n$ .

**Output:**  $(\mu_n^*, m_n^*, C_n^*) \in \mathbb{R}^{2p+p^2}$ , at any time  $n$  (or rank  $M$  version of the latter).

---

as above. It may also be of interest in an offline scenario to build up a database of labeled data and revise the emulator as this is done. Such a task is called experimental design, and greedy or myopic sequential experimental design can be posed elegantly within the sequential framework above.

### 3.2 Learning hyperparameters

Here we define the vector of parameters  $\phi = (\gamma^2, \nu, \delta^2, \lambda^2)$  to be optimized. Some of these may be fixed, but this provides a general framework. In particular, when some parameters are fixed the objective function may be convex or even analytically soluble. Nonetheless, we will consider global optimization for a 4 parameter objective function a solved problem and present the general method.

For parameter estimation, we introduce an *iterated nested VBEM algorithm*, which works as follows. For each  $\tau = 1, \dots$  the inner VBEM algorithm is as in (19) and Algorithm 1, and yields

$$q^{t,\tau}(\beta|\phi^\tau) \rightarrow q^{*,\tau}(\beta|\phi^\tau) = N(m_n^{*,\tau}, C_n^{*,\tau}).$$

This is then used in an outer standard EM on  $\phi$  to find

$$\phi^{\tau+1} = \operatorname{argmax}_\phi \int \log q^{*,\tau}(\beta, Y|\phi) q^{*,\tau}(\beta|Y, \phi^\tau) d\beta.$$

The details of how this is done will be described in detail in Section 3.2.2 below. The procedure is iterated until convergence. A more computationally efficient variant on this is given by executing single steps of the outer and inner algorithm iteratively (hence only one index is needed):

$$\phi^{t+1} = \operatorname{argmax}_\phi \int \log q^t(\beta, Y|\phi) q^t(\beta|Y, \phi^t) d\beta. \quad (37)$$

One can alternatively augment the variational distribution with an additional factor  $q(\phi)$ , which is learned in an additional step after (19). This approach seems somewhat more elegant but it turns out to be messy for our model, and for that reason is not considered further.

Note that all these approaches discussed above can be easily incorporated into Algorithm 1 and Algorithm 2 as optional steps that change values of  $\phi$  in between the consecutive iterations of the main algorithm.

#### 3.2.1 Some preliminaries

Before describing the method, it will be useful to recall some basic results relating to

$$\mathbb{P}(\theta|\beta, \phi) = \mathcal{GIG}(\theta_j; \nu - 1/2, \sqrt{\delta^2 + \beta_j^2}, \lambda),$$

which can be found for instance in [1].

The general calculation for  $\mathcal{GIG}$  distributions (with  $\delta^2, \lambda^2 \neq 0$ ) which we need is

$$\mathbb{E}(\theta_j^{-1}|\beta_j, \phi) = \frac{\lambda}{\sqrt{\delta^2 + \beta_j^2}} \frac{K_{\nu+\frac{1}{2}}\left(\lambda\sqrt{\delta^2 + \beta_j^2}\right)}{K_{\nu-\frac{1}{2}}\left(\lambda\sqrt{\delta^2 + \beta_j^2}\right)} + \frac{1-2\nu}{\delta^2 + \beta_j^2}, \quad (38)$$

where  $K_\alpha(z)$  denotes the modified Bessel function of the second kind. Note  $\theta_n^{t+1} := 1/\mathbb{E}_t(\theta_{n,j}^{-1})$  as in (21) and (14). Important special cases with analytically tractable expressions include  $\nu = 1$  and  $\nu = 0$ , in which case

$$\frac{K_{\frac{3}{2}}(z)}{K_{\frac{1}{2}}(z)} = \frac{z+1}{z}, \quad \frac{K_{\frac{1}{2}}(z)}{K_{-\frac{1}{2}}(z)} = 1. \quad (39)$$



Evaluating the expressions above at  $z = \lambda\sqrt{\delta^2 + \beta_j^2}$  gives

$$\mathbb{E}(\theta_j^{-1}|\beta_j, \nu = 1) = \frac{\lambda}{\sqrt{\delta^2 + \beta_j^2}}, \quad \mathbb{E}(\theta_j^{-1}|\beta_j, \nu = 0) = \frac{\lambda}{\sqrt{\delta^2 + \beta_j^2}} + \frac{1}{\delta^2 + \beta_j^2}. \quad (40)$$

If  $\lambda = 0$ , as in the ST and Jeff cases, then the ratio in the first term of (38) and (40) is not defined. The resulting calculation shows that the first term vanishes, and so we require  $\nu < 1/2$ .

### 3.2.2 Detailed approach

As before,  $X$  and  $n$  will be suppressed where not needed. Assume we run the algorithm of Section 2.3.2 for a fixed value of the hyper-parameters  $\phi^\tau$ , resulting in a joint variational distribution

$$q^{*,\tau}(\beta, Y|\phi) = \mathbb{P}(Y|\beta, \gamma^2)N(\beta; 0, D(1/\theta^{*,\tau}(\phi))),$$

where  $q^{*,\tau}(\beta|Y, \phi) = N(\beta; m_n^{*,\tau}, C_n^{*,\tau})$  is the variational posterior associated to this joint, and all relevant information about  $\phi^\tau$  is now encoded by  $\theta^{*,\tau}(\phi)$ , which appears in  $m_n^{*,\tau}, C_n^{*,\tau}$  via (22), (23). In particular,  $(\theta^\tau(\phi))^{-1}$  is given in general by (38), or for the particular cases of  $\nu = 0$  and  $\nu = 1$  by (40). An EM step for the MLE of  $\phi$  is

$$Q(\phi|\phi^\tau) = \int \log(q^{*,\tau}(\beta, Y|\phi))q^{*,\tau}(\beta|Y, \phi^\tau)d\beta, \\ \phi^{\tau+1} = \operatorname{argmax}_\phi Q(\phi|\phi^\tau). \quad (41)$$

The objective function for  $\gamma^2$  is given by

$$f(\gamma^2) := -n \log \gamma + \frac{1}{2\gamma^2} (s_n - 2v_n^T m_n^{*,\tau} + \operatorname{tr}[A_n(C_n^{*,\tau} + m_n^{*,\tau}(m_n^{*,\tau})^T)]), \quad (42)$$

where the following can be computed recursively in an online scenario

$$A_n := X_n^T X_n, \quad v_n := X_n^T Y_n, \quad s_n := Y_n^T Y_n. \quad (43)$$

This can be optimized independently of the remaining variables, giving

$$(\gamma_n^{t+1})^2 = \frac{1}{n} \mathbb{E}_\tau |Y_n - X_n \beta|^2 = \frac{1}{n} (s_n - 2v_n^T m_n^{*,\tau} + \operatorname{tr}[A_n(C_n^{*,\tau} + m_n^{*,\tau}(m_n^{*,\tau})^T)]),$$

where the expectation is with respect to  $q^{*,\tau}(\beta|Y, \phi^\tau)$ . Note that in cases where  $n < p$ , one can use the identity

$$\operatorname{tr}[A_n(C_n^{*,\tau} + m_n^{*,\tau}(m_n^{*,\tau})^T)] = \operatorname{tr}[X_n C_n^{*,\tau} X_n^T] + |X_n m_n^{*,\tau}|^2.$$

These computations are easily adapted to the online case described in Section 3.1.

The objective function for  $\phi$  is also easily computed as

$$\sum_{j=1}^p (\mathbb{E}_\tau(\beta_j^2)/\theta_j^\tau(\phi) + \log(\theta_j^\tau(\phi))), \quad (44)$$

where we recall again that  $(\theta^\tau(\phi))^{-1}$  is given in general by (38), or for the particular cases of  $\nu = 0$  and  $\nu = 1$  by (40). We consider global optimization for 3 (or fewer) parameters of cheap-to-evaluate functions to be essentially a solved problem [35], e.g. via combination of basic local

optimizers [64] initialized with multiple dispersed initial conditions. The derivative and Hessian are available in closed form, which is useful.

Some particular cases are convex and/or even analytically soluble. For example, in the BL case of  $\nu = 1$  and fixed  $\delta \geq 0$ , one has

$$(\lambda^{\tau+1})^{-1} = \frac{1}{p} \sum_{j=1}^p (C_{n,jj}^{*,\tau} + (m_{n,j}^{*,\tau})^2) / \sqrt{\delta^2 + C_{n,jj}^{*,\tau} + (m_{n,j}^{*,\tau})^2}. \quad (45)$$

While in the case of  $\nu = 0$  and fixed  $\delta \geq 0$ , one has

$$(\lambda^{\tau+1})^{-1} = \frac{1}{p - \sum_{i=1}^p \frac{C_{n,jj}^{*,\tau} + (m_{n,j}^{*,\tau})^2}{(\delta^2 + C_{n,jj}^{*,\tau} + (m_{n,j}^{*,\tau})^2)}} \sum_{j=1}^p \frac{C_{n,jj}^{*,\tau} + (m_{n,j}^{*,\tau})^2}{\sqrt{\delta^2 + C_{n,jj}^{*,\tau} + (m_{n,j}^{*,\tau})^2}}. \quad (46)$$

Finally, the ST case of  $\lambda = 0$  and fixed  $\delta \geq 0$  leads to

$$(1 - 2\nu^{\tau+1})^{-1} = \frac{1}{p} \sum_{j=1}^p (C_{n,jj}^{*,\tau} + (m_{n,j}^{*,\tau})^2) / (\delta^2 + C_{n,jj}^{*,\tau} + (m_{n,j}^{*,\tau})^2). \quad (47)$$

It is reassuring to note that if  $\delta = 0$  then the scale factor  $1 - 2\nu^{\tau+1} \equiv 1$ , i.e.  $\nu^{\tau+1} \equiv 0$ , just as in the case of the scale-invariant Jeffrey's prior. In other words, if we generalize Jeffrey's to allow any  $\nu < 1/2$  then we would find that standard Jeffrey's is optimal.

Despite less attractive theoretical properties in comparison to the full VBEM, this is a clean and simple approach for optimizing the hyperparameters. The objective function (41) is convex and analytically soluble (for the cases above). An obvious issue is the nested EM algorithms, which is undesirable. Hence, the second option may be preferred, which is to simply iterate between a single iteration of (41) and a single iteration of VBEM, as described in (37).

## 4 Numerical Results

In this section we will explore the approach presented on some simulated and real data. Code which implements the methods is available at GitHub repository.<sup>1</sup>

### 4.1 Diabetes data set

Here we present the VBL model and compare to the Bayesian LASSO (BL) of [65]. We use the simple diabetes data set from [32], with  $n = 484$  and  $p = 10$ , which was used in [65]. The fully Bayesian methodology is quite expensive, and yet tractable for this very small problem, which allows us to compare our very cheap variational approach. In turn, the VBL is applicable for problems with several orders of magnitude larger values for  $n$  and  $p$ , where even the mightiest supercomputers will struggle to achieve the full Bayesian solution. The results are shown in Figure 3.

The estimates of hyperparameter  $\lambda$  for VBEM and EM models are obtained by respectively using the second approach from Section 3.2 with  $\nu = 1$  (45). The resulted hyperparameters  $(\gamma, \lambda)$  are given by  $(\hat{\gamma}_{\text{VBEM}}, \hat{\lambda}_{\text{VBEM}}) = (53.62, 0.0041)$ . For the BL we take the optimal value  $\hat{\lambda}_{\text{BL}} = 0.237$  for the BL selected by maximum marginal likelihood as in [65] for the model there, which has the following relationship to our model  $\hat{\lambda}_{\text{BL}}/\gamma = \lambda$ , i.e. they scale the parameter

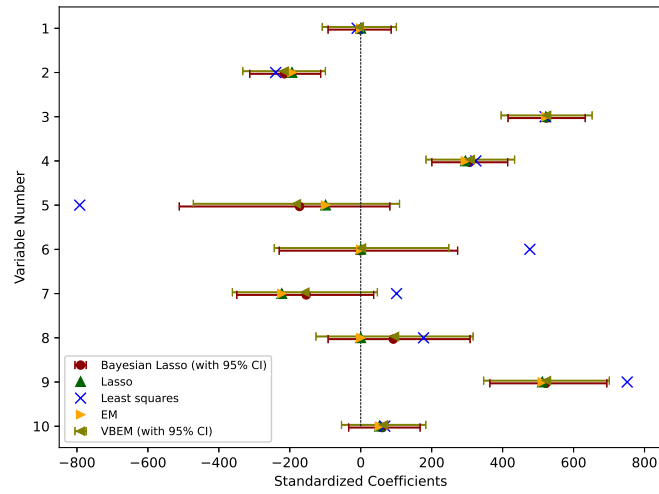
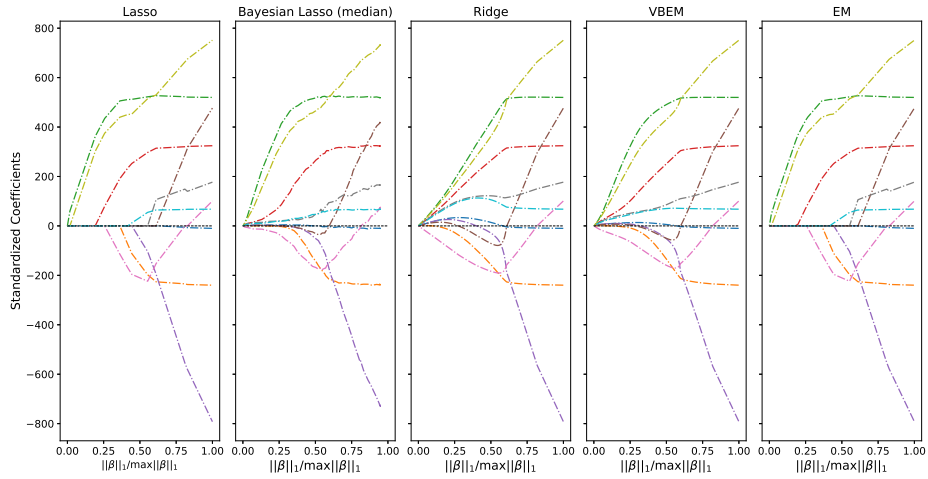


Figure 3: Illustration of the variational Bayesian LASSO (VBL) on the diabetes dataset. The top figure is analogous to Figure 1 of [65], except it adds VBL in the last 2 columns. The bottom one is analogous to Figure 2 of [65], except with VBL (and 95% credible interval) added.

in their model  $\hat{\lambda}$  by  $\gamma$ . See [60] for discussion of the benefits and drawbacks of the different formulations.

Another aspect of comparison between the BL and VBL (more precisely, the VBEM part) involves computational costs. Table 2 displays the inference time<sup>2</sup> (averaged over 30 runs) and the root-mean-squared error (obtained by 5-fold cross-validation) for VBEM and BL that were run with fixed hyperparameters  $\hat{\lambda}_{\text{VBEM}}$  and  $\hat{\lambda}_{\text{BL}}$ . The number of consecutive iterations of the BL Gibbs sampler is 10000 (after 1000 burn-in) as in [65], and the maximum number of iterations of the VBEM is limited by 10. It is worth highlighting that while the RMSEs are very similar (and correspond well with the noise estimation  $\hat{\gamma}_{\text{VBEM}}$  or  $\hat{\gamma}_{\text{EM}}$ ) the difference in inference time reaches an impressive 1000 times speed up.

	Time, ms	RMSE
VBEM, $\gamma \cdot \lambda = 0.220$	7.6 $\pm$ 0.7	54.611
BL, $\lambda = 0.237$	7560 $\pm$ 602	54.612

Table 2: VBEM and BL inference time and cross-validation errors.

## 4.2 Variable-selection: comparison of various examples with competitors

Next, we consider the toy model of [5], which is meant to assess skills in variable selection. As in [5], we set  $n = 100$  and  $p = 1000$  in (1). Then, we sample the design matrix  $X$  from zero-mean multivariate Gaussian distribution  $N(0_p, \Sigma)$ . The covariance matrix  $\Sigma$  is a block-diagonal one  $\Sigma = \text{bdiag}(\tilde{\Sigma}, \dots, \tilde{\Sigma})$  with blocks  $\tilde{\Sigma} = \{\tilde{\gamma}\}_{i,j=1}^{50}$ , where  $\tilde{\gamma}_{ij} = 1$  if  $i = j$  and  $\tilde{\gamma}_{ij} = 0.9$  otherwise. The true sparse vector of coefficients  $\beta^{\text{true}}$  is defined as  $\beta_i^{\text{true}} = \{-3.5, -2.5, -1.5, 1.5, 2.5, 3.5\}$  for  $i \in \{1, 51, 101, 151, 201, 251\}$  and zeros in all remaining  $(p - 6)$  positions. The response vector  $y$  is generated according to (1), where we set  $\gamma^2 = 3$ .

We compare the 5 choices of N-GIG priors given in Table 1 against the SSLASSO (mixture of LASSOs) [5], Sparse VB (mean-field variational spike and slab) [70], Horseshoe [19], variational Bayesian Bridge (for  $r \approx 0$ ) [3], and automatic differentiation variational Bayes (ADVI) for ST (inverse Gamma mixing distribution, but without a priori specified factorization) [51]. The competing methods were applied using the corresponding R packages: `SSLASSO`, `sparsevb`, `horseshoe`, `BayesBridge`, and `rstan` (R interface to probabilistic programming language Stan for ADVI method). The experiment was repeated 100 times, where each time we generated a new design matrix  $X$  and the corresponding vector of responses  $y$ . During each experiment, we tracked the following quantities.

- Mean squared error (MSE) and mean prediction error (MPE), defined as

$$\text{MSE} = \frac{1}{p} \|\hat{\beta} - \beta^{\text{true}}\|_2^2 \quad \text{and} \quad \text{MPE} = \frac{1}{n} \|X(\hat{\beta} - \beta^{\text{true}})\|_2^2,$$

where  $\hat{\beta}$  is corresponding point estimator of  $\beta|\mathcal{D}$ , and  $\beta^{\text{true}}$  is the frequentist truth defined above, which is used to simulate the data.

- The false discovery rate (FDR) and the false negative rate (FNR)

$$\text{FDR} = \frac{\text{FP}}{\text{FP} + \text{TP}} \quad \text{and} \quad \text{FNR} = \frac{\text{FN}}{\text{FN} + \text{TP}},$$

<sup>1</sup><https://github.com/zankin/SOVBR>

<sup>2</sup>This comparison was made on the laptop with Intel I7-7700HQ processor

where TP, TN, FP, and FN denote the number of true positives, true negatives, false positives, and false negatives, respectively. Positive means a discovery that the null hypothesis is false with 95% probability, where the null hypothesis is that  $\beta_j = 0$ , i.e. a positive refers to the discovery of a covariate or selection of the variable  $\beta_j \neq 0$ .

- Empirical coverage (EC) for the individual coefficients:

$$\text{EC} = \frac{1}{p} \sum_{j=1}^p \mathbb{1}_{A_j}(\beta_j^{\text{true}}),$$

where  $A_j$  is the 95% posterior credible interval,  $\mathbb{1}$  is an indicator function, and  $\beta_j^{\text{true}}$  is the frequentist truth used to simulate the data. For the examples which deliver Gaussian approximations  $N(m, C)$ , this is given by

$$A_j = (m_j - 2\sqrt{C_{jj}}, m_j + 2\sqrt{C_{jj}}).$$

For the MCMC examples, it is calculated based on the order statistics of the MCMC simulations  $\beta^{(i)}$ ,  $i = 1, \dots, N$ , as  $A_j = (a_{\min}^j, a_{\max}^j)$ , where

$$\frac{1}{N} \sum_{i=1}^N \mathbb{1}_{\{\beta_j^{(i)} < a_{\min}^j\}} = 0.025, \quad \text{and} \quad \frac{1}{N} \sum_{i=1}^N \mathbb{1}_{\{\beta_j^{(i)} > a_{\max}^j\}} = 0.025.$$

The results are presented in Table 3. Our method is faster than other VB methods, with better coverage and comparable accuracy. It is notable that the methods which achieve the best FDR and FNR have, respectively, worse FNR and FDR than our method. It, therefore, provides a nice balance of speed, UQ, and accuracy.

	MSE	MPE	FDR	FNR	Runtime, s	EC, %
BL (MAP)	0.009 (0.002)	0.701 (0.332)	0.006 (0.004)	0.183 (0.132)	2.44 (0.2)	-
BL (Mean)	0.012 (0.004)	0.832 (0.422)	0.009 (0.005)	0.145 (0.072)	2.44 (0.2)	99.42 (0.18)
Jeff (MAP)	0.006 (0.003)	0.743 (0.455)	0.007 (0.006)	0.220 (0.122)	2.72 (0.5)	-
Jeff (Mean)	0.011 (0.005)	0.923 (0.431)	0.011 (0.004)	0.110 (0.093)	2.72 (0.5)	99.49 (0.21)
ST (MAP)	<b>0.004 (0.002)</b>	0.623 (0.317)	0.004 (0.004)	0.183 (0.128)	2.57 (0.3)	-
ST (Mean)	0.007 (0.004)	0.651 (0.422)	0.006 (0.005)	0.110 (0.093)	2.57 (0.3)	<b>100.0 (0.00)</b>
NG (MAP)	0.011 (0.007)	0.770 (0.413)	0.009 (0.006)	0.145 (0.092)	3.01 (0.5)	-
NG (Mean)	0.016 (0.008)	0.801 (0.519)	0.012 (0.009)	0.122 (0.103)	3.01 (0.5)	99.30 (0.26)
NIG (MAP)	0.018 (0.006)	0.864 (0.317)	0.007 (0.006)	0.103 (0.092)	3.17 (0.4)	-
NIG (Mean)	0.022 (0.005)	0.983 (0.422)	0.013 (0.004)	0.081 (0.078)	3.17 (0.4)	99.40 (0.00)
SSLASSO	0.006 (0.006)	0.696 (0.552)	<b>0.001(0.001)</b>	0.171 (0.148)	<b>0.28(0.1)</b>	-
Sparse VB	0.016 (0.011)	1.497 (0.852)	0.007 (0.007)	0.335 (0.176)	4.52 (1.6)	99.38 (0.28)
Horseshoe	0.004 (0.005)	<b>0.619(0.446)</b>	0.047 (0.076)	0.030 (0.064)	47.3 (6.1)	99.88 (0.09)
BB (MAP)	0.030 (0.007)	2.732 (0.405)	0.046 (0.003)	0.166 (0.144)	4.72 (1.6)	-
BB (Mean)	0.016 (0.007)	4.669 (2.572)	0.318 (0.040)	0.033 (0.083)	206.6 (11.3)	99.67 (0.15)
ADVI (Stan)	0.026 (0.011)	2.993 (0.064)	0.166 (0.006)	<b>0.015(0.007)</b>	632.1 (25.7)	99.79 (0.11)

Table 3: MSE, MPE, FDR, FNR, Runtime, and Empirical Coverage (where relevant). For each quantity, we report average values across 100 experiments and corresponding standard deviations (in parentheses).

### 4.3 Total variation (TV) deblurring

Now we will consider the problem of image deconvolution. Consider that we would like to recover an image  $\tilde{\beta} \in \mathbb{R}^{\tilde{p}}$  comprised of  $\tilde{p} = p_0^2$  pixels, from observations  $Y = [y_1, \dots, y_n]^T \in \mathbb{R}^n$  with  $n \leq \tilde{p}$ . The design matrix is defined as follows, for  $l = 1, \dots, n$ ,

$$\tilde{x}_l^T \tilde{\beta} := z_{i_l, j_l}, \quad z = F^{-1} (D(\exp(-\omega|k|^2))) F \tilde{\beta}. \quad (48)$$

where  $\{(i_l, j_l)\}_{l=1}^n$  is a subset of pairs of indices associated to spatial observations of the degraded image/signal  $\tilde{\beta}$ , denoted  $z$  (both represented as 2 dimensional  $p_0 \times p_0$  arrays here),  $F$  denotes the discrete Fourier transform (which will be computed with fast Fourier transform (FFT) [23] at a cost of  $\mathcal{O}(p_0^2 \log p_0)$ ), and  $k = (k_1, k_2) \in \{-p_0/2, \dots, p_0/2 - 1\}^2$  is the multi-index of wave-numbers associated to the transformed signal. This simply corresponds to convolution in physical space with a Gaussian kernel with kernel width proportional to  $\omega$ . The observations are then defined as usual

$$y = \tilde{X}\tilde{\beta} + \epsilon, \quad \epsilon \sim N(0, \gamma^2 I_n).$$

Note that periodic boundary conditions are implicitly assumed once Fourier transform is used, however that constraint can be removed by padding with  $p_0$  additional zeros in each direction, sometimes referred to as *circulant embedding* [28].

Recall the discussion in Section 1.2. We now are interested not in sparse signals per se, but rather in edge-preservation, or in other words sparse gradient. For this purpose a popular choice is the (non-isotropic) total variation prior given by  $\prod_{j=1}^{p_0-1} \mathcal{L}((D_1\beta)_j; \lambda) \mathcal{L}((D_2\beta)_j; \lambda)$ , where  $D_i$  is some discrete approximation of the derivative with respect to coordinate  $j$ , for  $j = 1, 2$ . Often the finite difference is used, but here the natural choice is a Fourier approximation, given by  $D_j = F^{-1}(-i)k_j F$ ,  $i = \sqrt{-1}$ , and the missing degree of freedom corresponds to the constant wavenumber  $k = (0, 0)$ . This can be constructed as a marginal just like (10), using a pair of Normals  $\mathcal{N}((D_1\beta)_j; 0, \theta_j)$  and  $\mathcal{N}((D_2\beta)_j; 0, \theta_j)$  for each  $j = 1, \dots, \tilde{p} - 1$ . This change of variables proves to be messy within the VBEM (although it works just fine for EM/TV, even with a standard finite difference approximation in the spatial domain).

We adopt an alternative approach as follows, which we have found cleaner and more computationally expedient. Note that the TV prior can be alternatively written as a standard LASSO prior on  $\tilde{\beta} := \mathbf{D}\beta \in \mathbb{R}^{p-1}$ , where  $p = 2\tilde{p} + 1$  and  $\mathbf{D} = (D_1^T, D_2^T)^T \in \mathbb{R}^{p-1 \times \tilde{p}}$ . This matrix also has the vector  $\mathbf{1}_{\tilde{p}} \in \mathbb{R}^{\tilde{p}}$  of ones in its kernel. Denote the coefficient of  $\mathbf{1}_{\tilde{p}}$  as  $\beta_0$ . We can redefine the forward model on  $\beta := (\tilde{\beta}^T, \beta_0)^T$  as  $X := \tilde{X}(\mathbf{D}^\dagger, \mathbf{1}_{\tilde{p}})$ , where  $\mathbf{D}^\dagger = (\mathbf{D}^T \mathbf{D})^{-1} \mathbf{D}^T$  is the left pseudo-inverse of  $\mathbf{D}$ . Our data for the transformed model is

$$Y = X\beta + \epsilon. \tag{49}$$

Typically  $p_0$  will be large, for example  $p_0 = 256, 512$  or even larger, which precludes  $\mathcal{O}(p^2)$  calculations. In terms of computation, when  $n$  is small, then  $X^T$  can be computed explicitly with  $n$  FFTs, which allows explicit computation of  $G := C_0 X^T (X C_0 X^T + \gamma^2 I_n)^{-1}$  for small enough  $n$ . This allows computation of (8). In order to compute the diagonal of  $C_n$  in (9) we observe that the second term can be written as  $(G \circ (C_0 X^T)) \mathbf{1}_n$ , where  $\circ$  denotes the element-wise product of two matrices.

### 4.3.1 1D signal deblurring

Here we consider a simple 1D version, and compare VBL as well as the other models from Table 1 on the model data given by (49). The setting is exactly the same as described above, however  $D = 1$ , so there is a single index, 1D FFT, a single derivative,  $p = \tilde{p} + 1$ , and a discretization of  $\tilde{p} = p_0 = 200$  nodes are used between  $[-4, 24]$ . The signal is the 1D Bernholdt function  $f(s)$  for  $[-4, 10]$  [26], and padded with zeros on  $[10, 24]$ . Note that the domain has been doubled in order to accommodate non-periodic boundary conditions.

### 4.3.2 2D image deblurring

We now conduct several experiments on images. First we consider a toy model with  $n = \tilde{p} = p_0^2$  and  $p_0 = 28$ , with strong blurring and small noise. With a large  $\lambda$  we obtain very impressive

	BL (MAP)	Jeff (MAP)	ST (MAP)	BL (Mean)	Jeff (Mean)	ST (Mean)
MSE, $\times 1e^{-3}$	1.097	1.005	1.070	1.136	1.113	1.149
MPE, $\times 1e^{-6}$	3.903	3.461	3.506	4.020	3.623	3.689

Table 4: MSE and MPE errors for BL, Jeffreys, and ST priors.

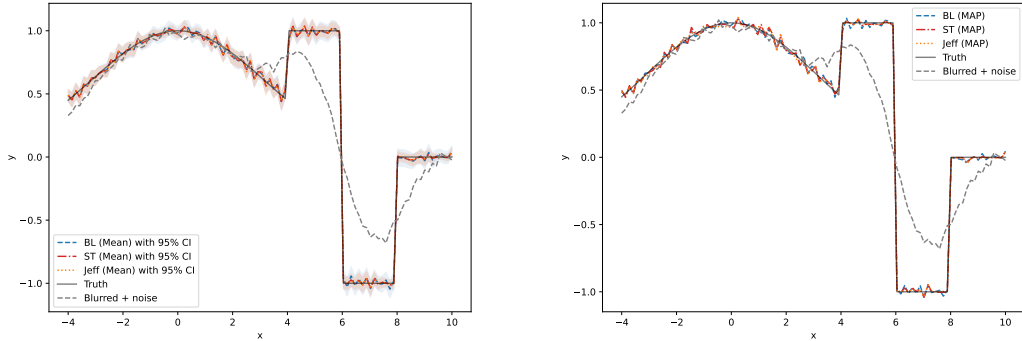


Figure 4: The plot shows the original function, blurred and noisy one, and the reconstructions obtained applying BL, Jeffreys, and ST priors.

reconstructions (see Figure 5). It is notable that the uncertainty is significantly underestimated, although relatively correct (in the sense that it is large and small where the error is). This is due to the fact that  $\lambda$  has been chosen too large, which, on the other hand, provides the impressive reconstruction of the edges. Notice here the top right-hand plot which shows the (relative  $L^2$ ) error as a function of iteration – its minimum may yield a much smaller error in comparison to the value at convergence, in particular for the MAP estimator (TV-EM). The plot also shows the data misfit, where we can observe the classical “L-curve” and see that an appropriate stopping criterion can be derived from convergence of the misfit (in the more realistic scenario where we do not know the error).

Now we will move to a higher dimensional example, with  $p_0 = 256$ . Observe that the case  $n = \tilde{p}$  cannot be handled directly, which provides a testing ground for our sequential method. However, it will be useful to have a ground truth, which is possible for appropriate choices of parameters. The calculation is provided in Appendix D. The first set of experiments in Figure 6 shows the reconstruction corresponding to full observations, and illustrates that VBL is capable of achieving edge sparsity as well as UQ.

The next set of experiments is intended to illustrate two things. First, in the case where the monolithic problem can be solved, as above, the sequential version does a good job of getting close to the full monolithic solution. For the choice of  $\omega = \gamma = 0.01$  and  $\lambda = 1$ , we recover a ground truth with  $\tilde{n} = 1514$  for  $\rho = 0.8$  (see Appendix D). The relative  $L^2$  error is 0.5. Letting  $2M = 1490$  for the recursive Algorithm 2, a single iteration of  $2M$  observations gives 0.58, while after completing the iterations, we get 0.52. The results are shown in Figure 7.

Second, in the case of smaller values  $\omega = \gamma = 0.001$  where the monolithic problem cannot be solved and one must settle for either sparse observations or a truncation of  $X$  above the desired threshold described in Appendix D, the sequential version does significantly better than the monolithic approximation. In this case, the desired threshold with  $\rho = 1$  would be  $\tilde{n} \approx 16000$  which is not feasible. We use the coarse approximation with  $\tilde{n} = 1640$  dominant modes, and



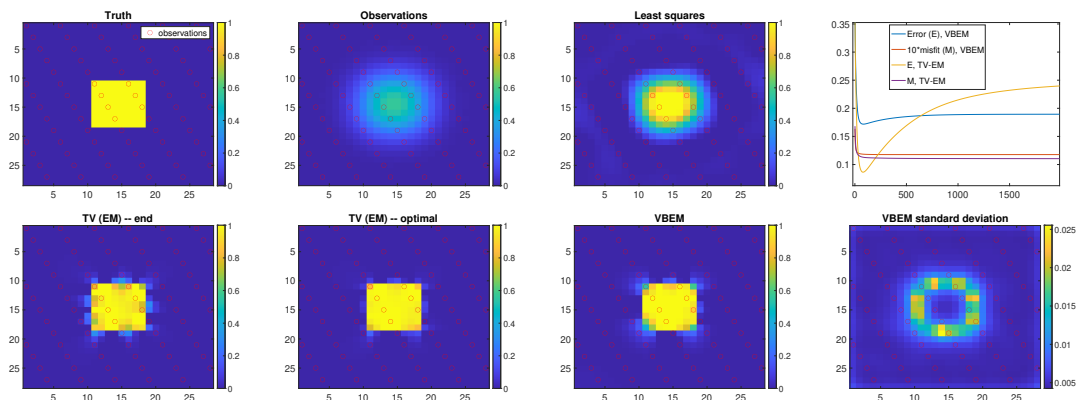


Figure 5: VBL TV-denoising illustrated on a simple toy image. The top row features (from left to right) the truth, blurry observations, the Tikhonov-regularized (least squares) solution, and a plot of the data misfit and reconstruction error over the EM/VBEM iterations for the various. The bottom row features (from left to right) the TV-regularized MAP estimator at convergence  $\mu_n$ , the TV-regularized MAP estimator at the minimum of the error (around iteration 100 – see top right), the VBL mean  $m_n$ , and the VBL standard deviation.

achieve relative  $L^2$  errors in the truncated observations of  $0.1 \gg \gamma$  and in the solution 0.39. For the recursive implementation we let  $2M = 1640$ , and achieve an error of 0.32. The results are shown in Figure 8. We notice in this case that, despite the fact that the reconstruction error is better and the edges are more crisp, there is some strange radiation/noise in the recursive reconstruction. It is a topic of further investigation to understand this better (and remove it).

The method is able to handle a larger problem with  $p = 10^6$  and we were able to assimilate  $n = 500$  batches of size  $M = 200$  overnight, reducing the relative error from 0.76 with a single pair of batches to 0.57 and yielding a reasonable looking reconstruction. These results are not shown.

**Remark 4.1** *Note that we impose a sparsity constraint on  $\beta_0$  as well, which is slightly different from TV. This constraint could be easily removed but our aim is not to belabour the finer points of TV-denoising and rather to illustrate our method on this example.*

## 5 Conclusion

Here a variational Bayesian approach is adopted for solution of Normal-Generalized-Inverse-Gaussian scale mixture models, which includes some existing and some new models. It is shown that the method delivers UQ at a cost much less than fully Bayesian models, as well as comparable accuracy and variable selection capabilities. The method is presented in a condensed and digestible form, and supplemented with an easy-to-implement code package, which will make this technology accessible to the wider science and engineering community. It is shown how it can be implemented online, which facilitates either batch processing of data or streaming data, for example in the context of sequential experimental design of computer simulations. Furthermore, an approximation is presented which is able to recover comparable results for a linear cost in the number of parameters  $p$ . The method is implemented on several real and simulated datasets, including a challenging high-dimensional image-deblurring example with  $p = 10^6$  and  $n = 10^5$ . It is compared with competing methods, where it is shown to perform favourably. In particular,

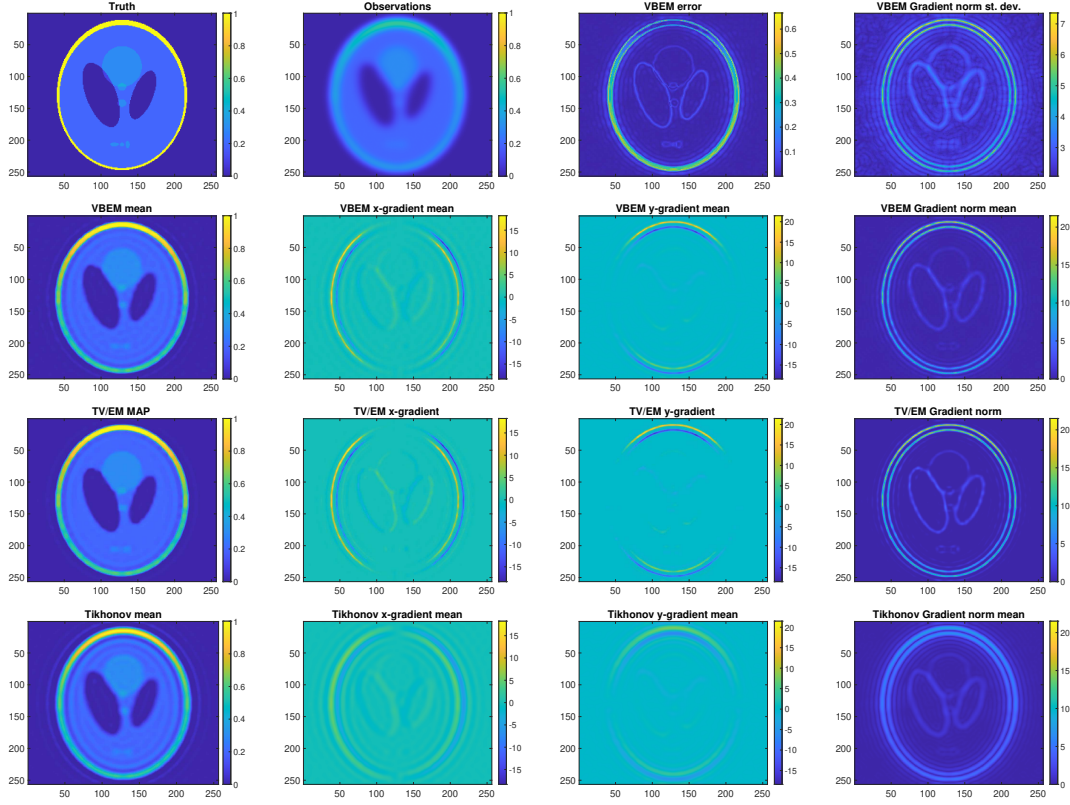


Figure 6: VBL TV-denoising illustrated on a high-resolution image of Shepp-Logan phantom. The top row features (from left to right) the truth, blurry observations (every pixel), the error w.r.t. VBL mean, and UQ in the form of the standard deviation of the gradient norm of VBL (i.e.  $(\mathbb{E}(\beta_{1:\bar{p}} - \mathbb{E}\beta_{1:\bar{p}})^2 + (\beta_{\bar{p}+1:2\bar{p}} - \mathbb{E}\beta_{\bar{p}+1:2\bar{p}})^2)^{1/2}$  – see the text). The second row features (from left to right) the VBL mean ( $\mathbb{E}\tilde{\beta}$ ), the x-gradient mean ( $\mathbb{E}\beta_{1:\bar{p}}$ ), the y-gradient mean ( $\mathbb{E}\beta_{\bar{p}+1:2\bar{p}}$ ), and the gradient mean norm ( $((\mathbb{E}\beta_{1:\bar{p}})^2 + (\mathbb{E}\beta_{\bar{p}+1:2\bar{p}})^2)^{1/2}$ ). The next two rows correspond to the same quantities for the TV MAP and the Tikhonov regularized problem.

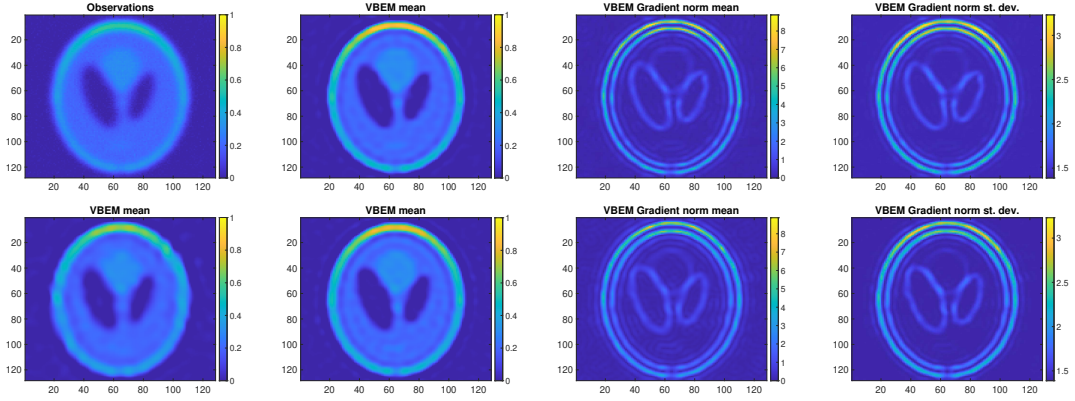


Figure 7: VBL TV-denoising (top row, from left to right – observations, mean, gradient mean, and gradient standard deviation) in comparison to the recursive version as in Algorithm 2 (bottom row, from left to right – mean after 1 iteration, mean, gradient mean, and gradient standard deviation).  $\omega = \gamma = 0.01$ .

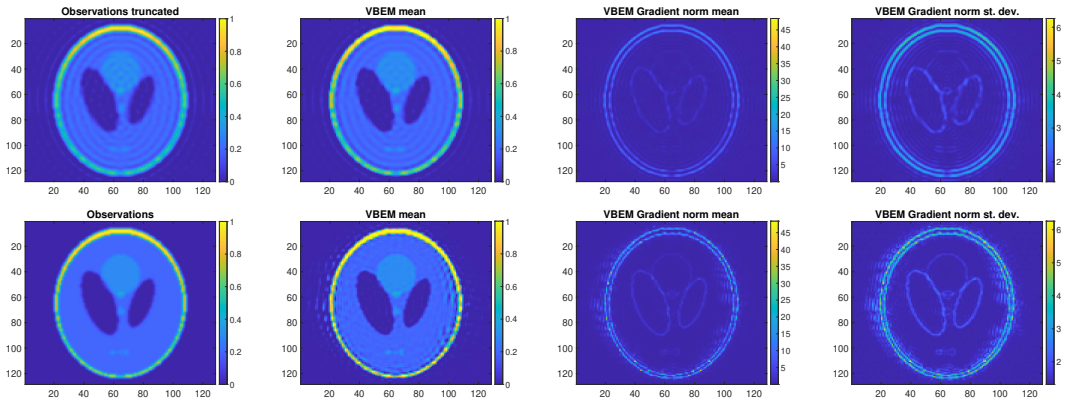


Figure 8: Truncated VBL TV-denoising (top row, from left to right – truncated observations, mean, gradient mean, and gradient standard deviation) in comparison to the recursive version as in Algorithm 2 (bottom row, from left to right – observations, mean, gradient mean, and gradient standard deviation).  $\omega = \gamma = 0.001$ .

it provides a nice balance of speed, accuracy, UQ, and ease-of-implementation. A parallel version will be presented in future work.

**Acknowledgements.** KJHL and VZ were supported by The Alan Turing Institute under the EPSRC grant EP/N510129/1. KJHL and VZ were also supported in part by the U. S. Department of Energy, Office of Science, Office of Fusion Energy Sciences and Office of Advanced Scientific Computing Research through the Scientific Discovery through Advanced Computing (SciDAC) project on Advanced Tokamak Modeling under a contract with Oak Ridge National Laboratory.

## References

- [1] Milton Abramowitz and Irene A Stegun. *Handbook of mathematical functions with formulas, graphs, and mathematical tables*, volume 55. US Government printing office, 1948.
- [2] David F Andrews and Colin L Mallows. Scale mixtures of normal distributions. *Journal of the Royal Statistical Society: Series B (Methodological)*, 36(1):99–102, 1974.
- [3] Artin Armagan. Variational bridge regression. In *Artificial Intelligence and Statistics*, pages 17–24. PMLR, 2009.
- [4] Hagai Attias. A variational Bayesian framework for graphical models. In *Advances in neural information processing systems*, pages 209–215, 2000.
- [5] Ray Bai, Veronika Rockova, and Edward I George. Spike-and-slab meets lasso: A review of the spike-and-slab lasso. *arXiv preprint arXiv:2010.06451*, 2020.
- [6] M. J. Beal and Z. Ghahramani. The variational Bayesian EM algorithm for incomplete data: with application to scoring graphical model structures. *Bayesian statistics*, 7(453-464):210, 2003.
- [7] Christopher M Bishop. *Pattern recognition and machine learning*. springer, 2006.
- [8] Christopher M Bishop and Michael E Tipping. Variational relevance vector machines. In *Proceedings of the Sixteenth conference on Uncertainty in artificial intelligence*, pages 46–53, 2000.
- [9] Niloy Biswas, Anirban Bhattacharya, Pierre E Jacob, and James E Johndrow. Coupled markov chain monte carlo for high-dimensional regression with half-t priors. *arXiv preprint arXiv:2012.04798*, 2020.
- [10] David M Blei, Alp Kucukelbir, and Jon D McAuliffe. Variational inference: A review for statisticians. *Journal of the American statistical Association*, 112(518):859–877, 2017.
- [11] George EP Box and George C Tiao. *Bayesian inference in statistical analysis*, volume 40. John Wiley & Sons, 2011.
- [12] Stephen Boyd, Neal Parikh, and Eric Chu. *Distributed optimization and statistical learning via the alternating direction method of multipliers*. Now Publishers Inc, 2011.
- [13] Kristian Bredies and Dirk A Lorenz. Linear convergence of iterative soft-thresholding. *Journal of Fourier Analysis and Applications*, 14(5-6):813–837, 2008.

- [14] David S Broomhead and David Lowe. Radial basis functions, multi-variable functional interpolation and adaptive networks. Technical report, Royal Signals and Radar Establishment Malvern (United Kingdom), 1988.
- [15] Gerrit Burgers, Peter Jan van Leeuwen, and Geir Evensen. Analysis scheme in the ensemble Kalman filter. *Monthly weather review*, 126(6):1719–1724, 1998.
- [16] Daniela Calvetti, Erkki Somersalo, and A Strang. Hierarchical Bayesian models and sparsity:  $L^2$ -magic. *Inverse Problems*, 35(3):035003, 2019.
- [17] François Caron, Luke Bornn, and Arnaud Doucet. Sparsity-promoting Bayesian dynamic linear models. 2012.
- [18] François Caron and Arnaud Doucet. Sparse Bayesian nonparametric regression. In *Proceedings of the 25th international conference on Machine learning*, pages 88–95, 2008.
- [19] Carlos M Carvalho, Nicholas G Polson, and James G Scott. The horseshoe estimator for sparse signals. *Biometrika*, 97(2):465–480, 2010.
- [20] Ismaël Castillo, Johannes Schmidt-Hieber, and Aad Van der Vaart. Bayesian linear regression with sparse priors. *The Annals of Statistics*, 43(5):1986–2018, 2015.
- [21] Scott Shaobing Chen, David L Donoho, and Michael A Saunders. Atomic decomposition by basis pursuit. *SIAM review*, 43(1):129–159, 2001.
- [22] Abdellah Chkifa, Albert Cohen, Giovanni Migliorati, Fabio Nobile, and Raul Tempone. Discrete least squares polynomial approximation with random evaluations- application to parametric and stochastic elliptic pdes. *ESAIM: Mathematical Modelling and Numerical Analysis*, 49(3):815–837, 2015.
- [23] James W Cooley and John W Tukey. An algorithm for the machine calculation of complex fourier series. *Mathematics of computation*, 19(90):297–301, 1965.
- [24] Ingrid Daubechies, Michel Defrise, and Christine De Mol. An iterative thresholding algorithm for linear inverse problems with a sparsity constraint. *Communications on Pure and Applied Mathematics: A Journal Issued by the Courant Institute of Mathematical Sciences*, 57(11):1413–1457, 2004.
- [25] Ingrid Daubechies, Ronald DeVore, Massimo Fornasier, and C Sinan Güntürk. Iteratively reweighted least squares minimization for sparse recovery. *Communications on Pure and Applied Mathematics: A Journal Issued by the Courant Institute of Mathematical Sciences*, 63(1):1–38, 2010.
- [26] David L. Green Jin M. Park Kody J. H. Law Clement Etienam David E. Bernholdt, Mark R. Cianciosa. Cluster, classify, regress: A general method for learning discontinuous functions. *Foundations of Data Science*, 1(4):491–506, 2019.
- [27] Arthur P Dempster, Nan M Laird, and Donald B Rubin. Maximum likelihood from incomplete data via the EM algorithm. *Journal of the Royal Statistical Society: Series B (Methodological)*, 39(1):1–22, 1977.
- [28] Claude R Dietrich and Garry N Newsam. Fast and exact simulation of stationary gaussian processes through circulant embedding of the covariance matrix. *SIAM Journal on Scientific Computing*, 18(4):1088–1107, 1997.

- [29] David L Donoho. Compressed sensing. *IEEE Transactions on information theory*, 52(4):1289–1306, 2006.
- [30] Arnaud Doucet, Nando de Freitas, and Neil Gordon. *Sequential Monte Carlo Methods in Practice*. Springer, 2001.
- [31] Jan Drugowitsch. Variational bayesian inference for linear and logistic regression. *arXiv preprint arXiv:1310.5438*, 2013.
- [32] Bradley Efron, Trevor Hastie, Iain Johnstone, Robert Tibshirani, et al. Least angle regression. *The Annals of statistics*, 32(2):407–499, 2004.
- [33] Geir Evensen. Sequential data assimilation with a nonlinear quasi-geostrophic model using Monte Carlo methods to forecast error statistics. *Journal of Geophysical Research: Oceans*, 99(C5):10143–10162, 1994.
- [34] Mário AT Figueiredo. Adaptive sparseness for supervised learning. *IEEE transactions on pattern analysis and machine intelligence*, 25(9):1150–1159, 2003.
- [35] Christodoulos A Floudas and Panos M Pardalos. *State of the art in global optimization: computational methods and applications*, volume 7. Springer Science & Business Media, 2013.
- [36] Daniel Gabay and Bertrand Mercier. A dual algorithm for the solution of nonlinear variational problems via finite element approximation. *Computers & mathematics with applications*, 2(1):17–40, 1976.
- [37] Stuart Geman, Elie Bienenstock, and René Doursat. Neural networks and the bias/variance dilemma. *Neural computation*, 4(1):1–58, 1992.
- [38] Tolstov P Georgi. Fourier series, 1976.
- [39] Roger Ghanem, David Higdon, and Houman Owhadi. *Handbook of uncertainty quantification*, volume 6. Springer, 2017.
- [40] Robert Mansel Gower, Nicolas Loizou, Xun Qian, Alibek Sailanbayev, Egor Shulgin, and Peter Richtárik. Sgd: General analysis and improved rates. In *International Conference on Machine Learning*, pages 5200–5209. PMLR, 2019.
- [41] Peter J Green, Krzysztof Łatuszyński, Marcelo Pereyra, and Christian P Robert. Bayesian computation: a summary of the current state, and samples backwards and forwards. *Statistics and Computing*, 25(4):835–862, 2015.
- [42] Jim E Griffin and Philip J Brown. Bayesian hyper-lassos with non-convex penalization. *Australian & New Zealand Journal of Statistics*, 53(4):423–442, 2011.
- [43] Ling Guo, Akil Narayan, and Tao Zhou. Constructing least-squares polynomial approximations. *SIAM Review*, 62(2):483–508, 2020.
- [44] Magnus Rudolph Hestenes, Eduard Stiefel, et al. *Methods of conjugate gradients for solving linear systems*, volume 49. NBS Washington, DC, 1952.
- [45] Arthur E Hoerl and Robert W Kennard. Ridge regression: Biased estimation for nonorthogonal problems. *Technometrics*, 12(1):55–67, 1970.

- [46] Paul W Holland and Roy E Welsch. Robust regression using iteratively reweighted least-squares. *Communications in Statistics-theory and Methods*, 6(9):813–827, 1977.
- [47] David R Hunter and Kenneth Lange. A tutorial on MM algorithms. *The American Statistician*, 58(1):30–37, 2004.
- [48] S Kaczmarz. Angenaherte auflosung von systemen linearer glei-chungen. *Bull. Int. Acad. Pol. Sic. Let., Cl. Sci. Math. Nat.*, pages 355–357, 1937.
- [49] Rudolph Emil Kalman. A new approach to linear filtering and prediction problems. *Journal of Basic Engineering*, 82(1):35–45, 1960.
- [50] Abbas Khalili and Jiahua Chen. Variable selection in finite mixture of regression models. *Journal of the american Statistical association*, 102(479):1025–1038, 2007.
- [51] Alp Kucukelbir, Rajesh Ranganath, Andrew Gelman, and David M Blei. Automatic variational inference in stan. *arXiv preprint arXiv:1506.03431*, 2015.
- [52] Harold Kushner and G George Yin. *Stochastic approximation and recursive algorithms and applications*, volume 35. Springer Science & Business Media, 2003.
- [53] Matti Lassas and Samuli Siltanen. Can one use total variation prior for edge-preserving Bayesian inversion? *Inverse Problems*, 20(5):1537, 2004.
- [54] Kody Law, Andrew Stuart, and Kostas Zygalakis. Data assimilation. *Cham, Switzerland: Springer*, 2015.
- [55] Felix Lucka. Fast Markov chain Monte Carlo sampling for sparse Bayesian inference in high-dimensional inverse problems using L1-type priors. *Inverse Problems*, 28(12):125012, 2012.
- [56] David JC MacKay. Bayesian methods for backpropagation networks. In *Models of neural networks III*, pages 211–254. Springer, 1996.
- [57] Markku Markkanen, Lassi Roininen, Janne MJ Huttunen, and Sari Lasanen. Cauchy difference priors for edge-preserving bayesian inversion. *Journal of Inverse and Ill-posed Problems*, 27(2):225–240, 2019.
- [58] Toby J Mitchell and John J Beauchamp. Bayesian variable selection in linear regression. *Journal of the american statistical association*, 83(404):1023–1032, 1988.
- [59] PD Moral. *Feynman-Kac formulae: Genealogical and interacting particle systems with applications, Probability and its applications*. Springer, New York, 2004.
- [60] Gemma E Moran, Veronika Ročková, and Edward I George. Variance prior forms for high-dimensional bayesian variable selection. *Bayesian Analysis*, 14(4):1091–1119, 2019.
- [61] Peter Müller and Fernando A Quintana. Nonparametric Bayesian data analysis. *Statistical science*, pages 95–110, 2004.
- [62] Radford M Neal. *Bayesian learning for neural networks*, volume 118. Springer Science & Business Media, 1996.
- [63] Sarah E Neville, John T Ormerod, and MP Wand. Mean field variational bayes for continuous sparse signal shrinkage: pitfalls and remedies. *Electronic Journal of Statistics*, 8(1):1113–1151, 2014.



- [64] Jorge Nocedal and Stephen Wright. *Numerical optimization*. Springer Science & Business Media, 2006.
- [65] Trevor Park and George Casella. The Bayesian LASSO. *Journal of the American Statistical Association*, 103(482):681–686, 2008.
- [66] Marcelo Pereyra. Proximal Markov chain Monte Carlo algorithms. *Statistics and Computing*, 26(4):745–760, 2016.
- [67] Marcelo Pereyra. Maximum-a-posteriori estimation with Bayesian confidence regions. *SIAM Journal on Imaging Sciences*, 10(1):285–302, 2017.
- [68] Nicholas G Polson, James G Scott, and Jesse Windle. The bayesian bridge. *Journal of the Royal Statistical Society: Series B: Statistical Methodology*, pages 713–733, 2014.
- [69] Ali Rahimi, Benjamin Recht, et al. Random features for large-scale kernel machines. In *NIPS*, volume 3, page 5. Citeseer, 2007.
- [70] Kolyan Ray and Botond Szabó. Variational bayes for high-dimensional linear regression with sparse priors. *Journal of the American Statistical Association*, pages 1–12, 2021.
- [71] Christian Robert and George Casella. *Monte Carlo statistical methods*. Springer Science & Business Media, 2013.
- [72] Veronika Ročková and Edward I George. The spike-and-slab lasso. *Journal of the American Statistical Association*, 113(521):431–444, 2018.
- [73] Vivekananda Roy, Sounak Chakraborty, et al. Selection of tuning parameters, solution paths and standard errors for Bayesian lassos. *Bayesian Analysis*, 12(3):753–778, 2017.
- [74] Yousef Saad. Krylov subspace methods for solving large unsymmetric linear systems. *Mathematics of computation*, 37(155):105–126, 1981.
- [75] Dino Sejdinović, Christophe Andrieu, and Robert Piechocki. Bayesian sequential compressed sensing in sparse dynamical systems. In *2010 48th Annual Allerton Conference on Communication, Control, and Computing (Allerton)*, pages 1730–1736. IEEE, 2010.
- [76] Ralph C Smith. *Uncertainty quantification: theory, implementation, and applications*, volume 12. Siam, 2013.
- [77] Qifan Song and Faming Liang. Nearly optimal bayesian shrinkage for high dimensional regression. *arXiv preprint arXiv:1712.08964*, 2017.
- [78] Thomas Strohmer and Roman Vershynin. A randomized kaczmarz algorithm with exponential convergence. *Journal of Fourier Analysis and Applications*, 15(2):262–278, 2009.
- [79] David Strong and Tony Chan. Edge-preserving and scale-dependent properties of total variation regularization. *Inverse problems*, 19(6):S165, 2003.
- [80] Andrew M Stuart. Inverse problems: a Bayesian perspective. *Acta numerica*, 19:451–559, 2010.
- [81] Robert Tibshirani. Regression shrinkage and selection via the lasso. *Journal of the Royal Statistical Society: Series B (Methodological)*, 58(1):267–288, 1996.

- [82] Andrei Nikolaevich Tikhonov. On the solution of ill-posed problems and the method of regularization. In *Doklady Akademii Nauk*, volume 151, pages 501–504. Russian Academy of Sciences, 1963.
- [83] Michael E Tipping et al. The relevance vector machine. In *NIPS*, volume 12, 1999.
- [84] Curtis R Vogel and Mary E Oman. Iterative methods for total variation denoising. *SIAM Journal on Scientific Computing*, 17(1):227–238, 1996.
- [85] Zheng Wang, Johnathan M Bardsley, Antti Solonen, Tiangang Cui, and Youssef M Marzouk. Bayesian inverse problems with  $l_1$  priors: a randomize-then-optimize approach. *SIAM Journal on Scientific Computing*, 39(5):S140–S166, 2017.
- [86] Ian En-Hsu Yen, Ting-Wei Lin, Shou-De Lin, Pradeep K Ravikumar, and Inderjit S Dhillon. Sparse random feature algorithm as coordinate descent in hilbert space. In *Advances in Neural Information Processing Systems*, pages 2456–2464. Citeseer, 2014.
- [87] Hao Zhu, Geert Leus, and Georgios B Giannakis. Sparsity-cognizant total least-squares for perturbed compressive sampling. *IEEE Transactions on Signal Processing*, 59(5):2002–2016, 2011.

## A Derivations related to EM

Following from (12), note that (i)  $Q(\beta|\beta^t) \leq \log \mathbb{P}(Y, \beta)$  and (ii)  $Q(\beta^t|\beta^t) = \log \mathbb{P}(Y, \beta^t)$ . Therefore

$$\begin{aligned}
 \log \mathbb{P}(Y, \beta^{t+1}) &= Q(\beta^{t+1}|\beta^t) + \log \mathbb{P}(Y, \beta^{t+1}) - Q(\beta^{t+1}|\beta^t) \\
 &\geq Q(\beta^{t+1}|\beta^t) \\
 &= Q(\beta^{t+1}|\beta^t) - Q(\beta^t|\beta^t) + \log \mathbb{P}(Y, \beta^t) \\
 &\geq \log \mathbb{P}(Y, \beta^t).
 \end{aligned}$$

The first inequality arises from property (i), the equality comes from property (ii) and the final inequality is due to the optimality of  $\beta^{t+1}$ . This shows that the EM algorithm provides a non-decreasing algorithm for the optimization of  $\log \mathbb{P}(Y, \beta^{t+1})$ . It is a particular case of what have come to be known as majorization minimization algorithms [47].

The full calculation of (13) is given by

$$\begin{aligned}
 Q(\beta|\beta^t) &:= - \int \log(\mathbb{P}(\beta, Y_n|\theta, X_n))\mathbb{P}(\theta|\beta^t, X_n, Y_n)d\theta + \kappa(\beta^t, X_n, Y_n) \\
 &= - \int (\log(\mathbb{P}(\beta|\theta)) + \log(\mathbb{P}(Y_n|\beta, X_n))) \mathbb{P}(\theta|\beta^t, X_n, Y_n)d\theta + \kappa(\beta^t, X_n, Y_n) \\
 &= \frac{1}{2} \sum_j \beta_j^2 \mathbb{E} \left[ \frac{1}{\theta_j} \middle| \beta^t, X_n, Y_n \right] + \frac{1}{2} \mathbb{E} \left[ \log(\theta_j) \middle| \beta^t, X_n, Y_n \right] + \frac{1}{2\gamma^2} |Y_n - X_n\beta|_2^2 + \kappa(\beta^t, X_n, Y_n) \\
 &= \frac{1}{2} \beta^T D(1/\theta^t)\beta + \frac{1}{2\gamma^2} |Y_n - X_n\beta|_2^2 + \kappa(\beta^t, X_n, Y_n),
 \end{aligned}$$

where  $\kappa$  is a generic constant which changes from line to line and absorbs all irrelevant terms.

## B Discussion of other iterative methods for MAP estimation

It is worth briefly discussing other standard iterative optimization algorithms for solving quadratic optimization problems. In particular, gradient descent and quasi-Newton methods are very promising alternatives in the case where the design matrix  $X_n$  is sparse. This is not the primary context of interest in the present work, so the general case is discussed. Gradient descent methods achieve *linear convergence*, which means that in terms of iterations the complexity is logarithmic in the desired accuracy [64], however the rate can get very close to one, particularly in high dimensions, resulting in very slow convergence in practice. Computation of the gradient incurs a cost of  $\mathcal{O}(np)$ , and if one uses a conjugate gradient approach [64, 44] (ensuring that each successive search direction is orthogonal to all previous ones) then the number of iterations required for convergence to *the exact solution* is bounded above by  $p$ , i.e. the memory and computational complexity is no worse than the monolithic approach. Stochastic gradient descent alleviates  $n$ -dependence per iteration by using an unbiased estimate of the gradient, i.e. a batch of  $b = \mathcal{O}(1)$  data is used at each iteration with a cost of  $\mathcal{O}(p)$ . Under appropriate assumptions, this approach can converge [52, 40], but there are no tight theoretical complexity bounds. In the machine learning literature, one often refers to *epochs*, or *sweeps* (plural) through the full data set, so one can expect a complexity of at least  $\mathcal{O}(np)$ . An alternative in similar spirit is the (randomized) Kaczmarz algorithm [48, 78], which also enjoys a per iteration cost of  $\mathcal{O}(p)$ , but would also typically require  $\mathcal{O}(n)$  iterations until convergence. The latter may be improved with a  $\mathcal{O}(np)$  pre-processing step which replaces a uniform distribution on the data with one scaled by the row norms of  $X_n$ .

Of course none of these methods provides an uncertainty estimate. Quasi-Newton methods, such as BFGS, provide an approximation of the covariance  $C_n$  from equations (9), (51) as well as super-linear convergence. In this case, one has a per iteration complexity cost of  $\mathcal{O}(p(n+p))$ , and a memory requirement of  $\mathcal{O}((n+2k)p)$ , for  $k$  iterations (a rank 2 update to the approximation of the Hessian and its inverse is performed at each iteration). The limited memory alternative limits  $k \leq k_{\max}$ . One expects the method to converge very rapidly, for  $k = \mathcal{O}(1)$ , so it can still be competitive. A one-off cost of  $\mathcal{O}(np^2)$  to compute  $X_n^T X_n$  and  $X_n^T Y_n$  can reduce the  $n$ -dependence of either method to a  $p$ -dependence. Furthermore, the computation of  $X_n^T X_n$  can be split into  $n/m$  batches of size  $m$  to be computed in parallel, yielding  $\mathcal{O}(mp)$  memory and  $\mathcal{O}(p^2 m)$  computation cost for each, for the price of an additional  $\mathcal{O}(p^2 n/m)$  cost to combine at the end.

## C Ensemble Kalman filter formulation

In an online context, the Kalman filter provides recursive equations below, analogous to (8) and (9), for either the covariance or the precision

$$\begin{aligned} m_n &= \left( \frac{1}{\gamma^2} x_n x_n^T + C_{n-1}^{-1} \right)^{-1} \left( \frac{1}{\gamma^2} x_n y_n + C_{n-1}^{-1} m_{n-1} \right) \\ &= m_{n-1} + C_{n-1} x_n (\gamma^2 + x_n^T C_{n-1} x_n)^{-1} (y_n - x_n^T m_{n-1}), \end{aligned} \quad (50)$$

$$C_n = \left( \frac{1}{\gamma^2} x_n x_n^T + C_{n-1}^{-1} \right)^{-1} = C_{n-1} - C_{n-1} x_n (\gamma^2 + x_n^T C_{n-1} x_n)^{-1} x_n^T C_{n-1}. \quad (51)$$

We have the following incremental update formula for (23), which incurs a cost of  $\mathcal{O}(p)$

$$(C_n^\theta)^{-1} = (C_n^{\theta'})^{-1} - D(1/\theta') + D(1/\theta). \quad (52)$$

Unfortunately, the solution of (22) requires inversion of a  $p \times p$  to compute (50), at a premium cost of  $\mathcal{O}(p^3)$  (for exact solution and in the absence of sparsity).

In this context it is natural to consider the ensemble Kalman filter as a low-rank and cost-efficient alternative. The EnKF was introduced in [33, 15] and has since exploded in popularity, largely due to its remarkable success in providing an efficient approximation to the Kalman filter in very high dimensional geophysical applications. Many versions of EnKF exist, but in this case the version which makes the most sense is the deterministic, or square root, EnKF [54]. The method is initialized with an ensemble  $\beta_0^{(1)}, \dots, \beta_0^{(K)} \sim N(m_0, C_0)$ , and then the Kalman filter equations (50) are replaced with the following, for  $n \geq 1$

$$\begin{aligned} m_{n-1} &= \frac{1}{K} \sum_{i=1}^K \beta_{n-1}^{(i)}, & C_{n-1} &= \frac{1}{K} \sum_{i=1}^K (\beta_{n-1}^{(i)} - m_{n-1})(\beta_{n-1}^{(i)} - m_{n-1})^T, \\ \widehat{m}_n &= m_{n-1} + C_{n-1} x_n (\gamma^2 + x_n^T C_{n-1} x_n)^{-1} (y_n - x_n^T m_{n-1}), \\ \widehat{C}_n &= (I_p - C_{n-1} x_n (\gamma^2 + x_n^T C_{n-1} x_n)^{-1}) C_{n-1}, \\ \beta_n^{(i)} &\sim \mathcal{N}(\beta; \widehat{m}_n, \widehat{C}_n), \quad i = 1, \dots, K, \end{aligned} \quad (53)$$

The most common regime of application is  $K \ll p$ , which admittedly looks dubious from a statistical perspective. However, the cost of this method is now  $\mathcal{O}(Kp)$  in both computation and memory, so the impetus is clear from a purely computational perspective. The remarkable thing is that it actually often works quite well, although we note that the more common regime of application is dynamical systems in which some particle-wise (often nonlinear) forward propagation occurs in between (54) and (53). The stochastic version can be used directly in the absence of the sparsity considerations of Section 1.2. However, in order to use the identify (52) we need the precision. One potential, and common, solution is to modify/inflate (53) for some small  $\epsilon > 0$  with

$$C_n = \frac{1}{K} \sum_{i=1}^K (\beta_n^{(i)} - m_n)(\beta_n^{(i)} - m_n)^T + \epsilon I_p. \quad (55)$$

In our case, however, there is by design a more sensible choice of approximation by a diagonal matrix plus low-rank correction. The whole program can be carried out, but due to this fact, we will not consider EnKF further here. Note that such adjustments, known generally as covariance inflation in the data assimilation literature [54], prevent convergence of the model to the Kalman filter in the limit of an infinite sample size, so exactness is lost.

## D Full observations Fourier truncation for TV denoising

Thanks to the diagonalization of  $\tilde{X}$  we can identify an approximation as follows. Let  $\mathcal{I} := \{k; \exp(-\omega|k|^2) > \rho\gamma\}$ , for  $\rho < 1$ , such that for  $z = \tilde{X}\tilde{\beta}$  and  $\widehat{z} = \tilde{X}_{\mathcal{I}}\tilde{\beta}$ , we have  $|z - \widehat{z}| < \gamma$ , i.e. the observed signal is less than the observational noise. Here  $\tilde{X}_{\mathcal{I}}$  is shorthand notation for the rank  $\tilde{n} = |\mathcal{I}|$  approximation of  $\tilde{X}$  obtained by truncating wavenumbers  $k \notin \mathcal{I}$ . For appropriate choices of  $\omega, \gamma > 0$ , this provides a tractable scenario for full observations (in the sense that the solution is close to the actual full observation case). The situation is slightly complicated however, since  $X \in \mathbb{R}^{\tilde{p} \times p}$  despite being rank  $\tilde{n}$ . We therefore approximate  $X \approx X_{\ell} X_r$ , where  $X_{\ell} \in \mathbb{C}^{\tilde{p} \times \tilde{n}}$  and  $X_r \in \mathbb{C}^{\tilde{n} \times p}$  are defined as follows

$$X_{\ell} := F^{-1}(\exp(-\omega|k|^2))_{k \in \mathcal{I}}, \quad X_r^{\dagger} := \begin{pmatrix} F^{-1}(ik_1|k|^{-2})_{k \in \mathcal{I}} \\ F^{-1}(ik_2|k|^{-2})_{k \in \mathcal{I}} \\ \tilde{p}\delta_{k=0} \end{pmatrix}.$$

Now  $X^\dagger X = X_r^\dagger (X_\ell^\dagger X_\ell) X_r$  and we simply redefine (9) with an alternative application of the Sherman Morrison Woodbury matrix identity

$$C_n = (I_p - \tilde{K} X_r) C_0, \quad \tilde{K} = C_0 X_r^\dagger (X_r C_0 X_r^\dagger + \gamma^2 (X_\ell^\dagger X_\ell)^{-1})^{-1},$$

and (8) becomes

$$m_n = \tilde{K} (X_\ell^\dagger X_\ell)^{-1} X_\ell^\dagger Y.$$

We note that  $X_\ell^\dagger X_\ell \in \mathbb{R}^{\tilde{n} \times \tilde{n}}$  can be easily computed and inverted for a cost  $\mathcal{O}(p\tilde{n}^2)$ .